HHS Public Access

Author manuscript

Cell Rep. Author manuscript; available in PMC 2023 October 23.

Published in final edited form as:

Cell Rep. 2023 February 28; 42(2): 112105. doi:10.1016/j.celrep.2023.112105.

Dipeptidylpeptidase 4 promotes survival and stemness of acute myeloid leukemia stem cells

Chen Wang[1,7], **Ravi Nistala**[1,2,7], **Min Cao**[1], **Yi Pan**[1], **Madelaine Behrens**[1], **Donald Doll**[3], **Richard D. Hammer**[4], **Puja Nistala**[3], **Hui-Ming Chang**[5,6], **Edward T.H. Yeh**[6], **XunLei Kang**[1,3,8,*]

[1]Center for Precision Medicine, Department of Medicine, University of Missouri School of Medicine, Columbia, MO 65212, USA

[2]Division of Nephrology, Department of Medicine, University of Missouri School of Medicine, Columbia, MO 65212, USA

[3]Division of Hematology and Oncology, Department of Medicine, University of Missouri School of Medicine, Columbia, MO 65212, USA

[4]Department of Pathology and Anatomical Sciences, University of Missouri School of Medicine, Columbia, MO 65212, USA

[5]Department of Pharmacology and Toxicology, The University of Arkansas for Medical Sciences, Little Rock, AR 72205, USA

[6]Department of Internal Medicine, The University of Arkansas for Medical Sciences, Little Rock, AR 72205, USA

[7]These authors contributed equally

[8]Lead contact

SUMMARY

Leukemic-stem-cell-specific targeting may improve the survival of patients with acute myeloid leukemia (AML) by avoiding the ablative effects of standard regimens on normal hematopoiesis. Herein, we perform an unbiased screening of compounds targeting cell surface proteins and identify clinically used DPP4 inhibitors as strong suppressors of AML development in both murine AML models and primary human AML cells xenograft model. We find in retrovirus-induced AML mouse models that DPP4-deficient AML cell-transplanted mice exhibit delay and reversal of AML development, whereas deletion of DPP4 has no significant effect on normal

*Correspondence: kangxu@health.missouri.edu.

AUTHOR CONTRIBUTIONS

Conceptualization, R.N. and X.K.; methodology, C.W., R.N., E.T.H.Y., H.-M.C., and X.K.; validation, M.C.; investigation, C.W., M.B., M.C., and X.K.; writing – original draft, R.N. and X.K.; writing – review & editing, R.N. and X.K.; data curation, C.W., R.D.H., and Y.P.; visualization, C.W. and X.K.; funding acquisition, R.N. and X.K.; resources, D.D., R.D.H., and X.K.; supervision, X.K.

SUPPLEMENTAL INFORMATION

Supplemental information can be found online at https://doi.org/10.1016/j.celrep.2023.112105.

DECLARATION OF INTERESTS

The authors declare no competing interests.

hematopoiesis. DPP4 activates and sustains survival of AML stem cells that are critical for AML development in both human and animal models via binding with Src kinase and activation of nuclear factor κB (NF-κB) signaling. Thus, inhibition of DPP4 is a potential therapeutic strategy against AML development through suppression of survival and stemness of AML cells.

Graphical Abstract

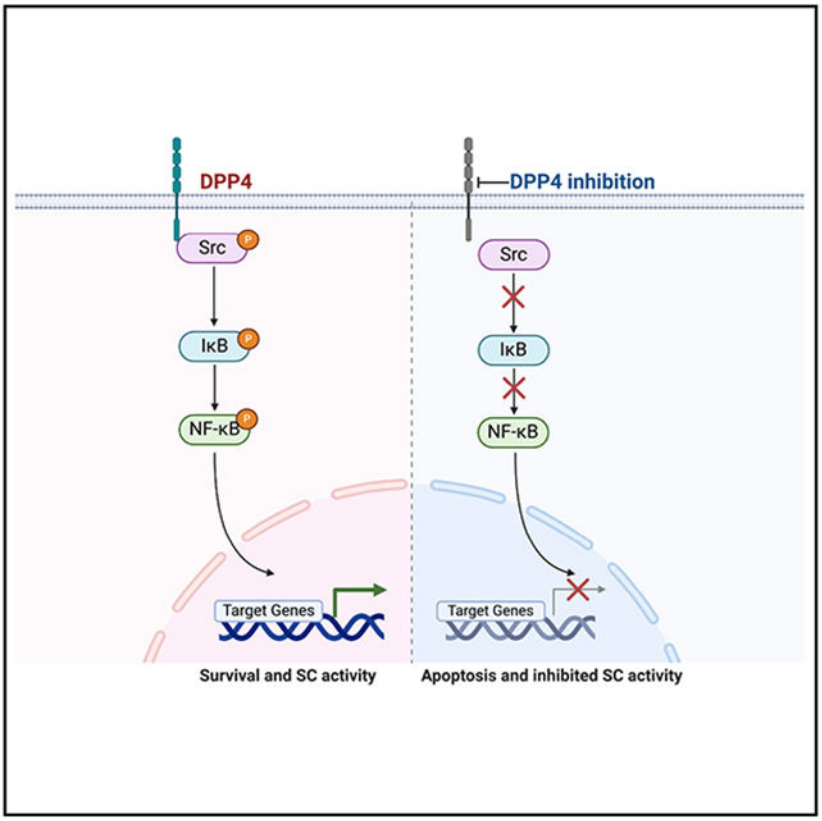

In brief

Chen et al. show that leukemic cells, when compared with normal hematopoietic stem cells, overexpress a cell surface protein called DPP4, which is essential for their survival and confers stemness. Currently available inhibitors of this cell surface protein exhibit potential as effective leukemia therapeutic agents.

INTRODUCTION

Acute myeloid leukemia (AML) is the most common acute leukemia in adults and is responsible for the highest number of annual deaths among leukemias in the United States. Recent advances have resulted in targeted therapies and low-intensity regimens tailored toward mutation-positive AML and subjects >65 years old, respectively.[1] Although the novel treatments significantly improve clinical outcome for some AML subsets, their benefit to a large proportion of patients has been limited. The overall prognosis remains poor with 5 year survival of only 29%. A major challenge in the field of AML therapy is that a

limited number of specific targets have been identified in AML cells. Moreover, most current treatments affect normal hematopoietic cells, resulting in significant adverse effects.[2] In this regard, standard chemotherapy with “cytarabine + anthra-cycline” or allogeneic hematopoietic stem cell transplant (alloSCT) is associated with significant morbidity and mortality.[3] Therefore, an effective yet tolerable therapy for AML is an urgent unmet need.

Cell surface proteins are important therapeutic targets due to their role as cell markers and their extracellular accessibility.[4] Importantly, the expression and function of these cell surface proteins and downstream signaling may differ in leukemia cells from those of normal hematopoietic cells.[5,6] We screened a group of compounds, which are thought to target cell surface proteins expressed in both human and mouse AML cells, and identified CD26/dipeptidylpeptidase 4 (DPP4), as a potential target for AML treatment. DPP4 exists primarily as a membrane-bound extracellular peptidase that cleaves Xaa-Pro or Xaa-Ala dipeptides from the N terminus of polypeptides.[7] DPP4 is expressed by many types of cells and in different organ systems, including the hematopoietic system.[8] DPP4 substrates G-CSF and C-X-C motif chemokine 12 (CXCL12) have been shown to play a role in the regulation of hematopoietic stem cell (HSC) trafficking.[9,10] DPP4 has been identified as a biomarker and target of leukemia stem cells for both chronic myeloid leukemia (CML) and acute lymphoblastic leukemia (ALL).[11-13] In contrast, DPP4-truncated granulocyte-macrophage colony-stimulating factor (GM-CSF) and interleukin-3 (IL-3) have been shown to inhibit normal and malignant hematopoiesis.[14] Recently, inhibition of DPP4 activity in AML exosomes was shown to reverse exosome-mediated myelosuppression.[15] Nevertheless, the function of DPP4 in AML cells and AML development is unknown. Herein, we demonstrate that inhibition or deletion of DPP4 suppressed AML development.

RESULTS

Growth of AML cells is dependent on DPP4

To identify potential cell surface targets that are effective for AML treatment, we explored compound libraries (MedChemExpress, #HY-L022, #HY-L026) for more than 1,200 compounds with clinical utility that target cell surface proteins and identified 57 candidate compounds to perform further phenotype-based *in vitro* screening (Figures 1A-1D and S1A). We tested the efficacy on cell growth in 3 human leukemic cell lines and inhibition of colony-forming unit ability (CFU) of primary mouse AML cells. We observed that linagliptin, a highly DPP4-specific inhibitor and a medication widely used in clinics for type two diabetes mellitus (T2DM), displayed the most significant and consistent suppression of growth of both human and mouse AML cells (Figures 1A-1D and S1B). To further assess the dependence of human AML (hAML) development on DPP4, we selected THP-1 cells, which consistently manifest the highest cell surface expression and enzyme activity of DPP4 among the human leukemic cell lines examined (Figures 1E and 1F). We found that both linagliptin and vildagliptin (another DPP4 inhibitor) significantly suppressed hAML cell growth by increasing apoptosis *in vitro* in a dose-dependent manner, with IC50s of 223.1 and 1,084.8 nM, respectively (Figures 1G, 1H, S1C, and S1D). In addition, two different short hairpin RNAs (shRNAs) independently and efficiently decreased total expression of DPP4 and essentially blocked the *in vitro* growth of AML cells, likely via significantly

increasing apoptosis of leukemia cells, but did not alter the cell-cycle status, which is consistent with the effects of DPP4 inhibitors (Figures 1I-1L and S1E).

DPP4 inhibitors suppress AML development, not the activity of HSCs and progenitors (HSPCs)

DPP4 is expressed on the majority of leukemic stem cell (LSC)-enriched populations, identified as $YFP^+Kit^+Mac1^+$ cells in the bone marrow (BM) of MLL-AF9 AML mice.[16] Furthermore, the more restricted AML stem cell (AML-SC) population in this model, GMP-like leukemic (L-GMP) cells ($YFP^+Lin^-Sca\text{-}1^-Kit^+CD34^+Fc\gamma RII/III^+$),[17] had increased levels of DPP4 expression when compared with normal GMP cells (YFP^- GMP) after MLL-AF9 transformation (Figure S2A), which is consistent with DPP4 being a SC biomarker similar to CML and ALL[11-13] (Figure 2A). Interestingly, DPP4 inhibitors significantly decrease CFU ability of primary mouse AML cell in a dose-dependent manner (Figures 2B and 2C) while not affecting that of normal BM cells (Figures 2D and 2E), in part due to the differences in inhibition of DPP4 enzyme activity (Figures 2C, 2E, and S2B). Next, we compared the efficacy of linagliptin with cytarabine (Ara-C), the mainstay induction therapy for most patients with AML, by treating mouse AML cells at various concentrations[18,19] and observed weak inhibition of cell growth at low concentrations of linagliptin (0.1–1 ng/mL) but similar treatment efficacy to Ara-C at higher concentrations (100–1,000 ng/mL) (Figure 2F).[16,17] In support of *in vitro* efficacy, 20 days of continuous treatment with linagliptin (1 mg/kg/day) led to significantly increased survival of AML cell-transplanted mice due to slower AML development, similar to Ara-C treatment (100 mg/kg/day over 5 days) (Figures 2G-2I). Furthermore, there were no common adverse drug effects (ADEs), such as hypoglycemia (Figure 2J) and BM suppression/myelosuppression indicated by SC activity of YFP^- BM cells (non-AML cells) (Figure 2K).

hAML growth is dependent on increased expression and activity of DPP4

Query of 3 human databases revealed that high expression of DPP4 was associated with reduced survival of patients with AML (Figures S3A-S3C). To examine whether high expression of DPP4 is essential for hAML development, we measured cell surface expression and enzyme activity of DPP4 and observed significantly higher levels in primary AML cells from human patients compared with peripheral blood (PB) myeloid cells from healthy controls (Figures 3A-3C and S3D). Furthermore, $CD34^+$ hAML blast cells express DPP4 at a significantly higher level than $CD34^+$ healthy controls or $CD34^-$ non-blast AML cells, indicating that DPP4 is specifically expressed higher in LSC-enriched AML cells (Figures 3D and 3E). Intriguingly, linagliptin treatment of high DPP4-expressing AML cells from 3 human patients significantly inhibited LSC activity and increased AML cell apoptosis (Figures 3F and 3G). To test whether DPP4 inhibitor is effective for AML treatment *in vivo*, we transplanted primary hAML cells to xenograft NOD/SCID-IL2RG (NSG) mice and treated the mice with linagliptin (Figure 3H). We observed that linagliptin treatment significantly reduced AML cell infiltration in PB after 30 days treatment (35.1% vs. 2.4%) and increased overall survival of the mice when compared with controls (vehicle treatment) (Figures 3I-3K). Together, these data support the premise that DPP4 inhibition significantly suppresses hAML development. Next, we investigated whether suppression of DPP4 expression of hAML cells alters *in vitro* LSC activity and *in vivo* AML cell growth in

transplanted NSG mice (Figure 3L). We observed greatly reduced CFU ability and increased apoptosis in DPP4-deficient hAML samples (Figures 3M and 3N). Transplantation of DPP4-deficient hAML cells into NSG mice suppressed leukemia development, as demonstrated by significantly prolonged overall survival and reduced engraftment of GFP^+ cells (marking the lentivirus-infected hAML cells) into BM, spleen, liver, and PB (Figures 3O-3R). These results demonstrate that DPP4 is essential for hAML development, which further supports the notion that high expression of DPP4 negatively correlates with the overall survival of patients with AML (Figures S3A-S3C).

Hematopoietic-cell-specific deletion of DPP4 does not affect normal hematopoiesis

We generated a hematopoietic-system-specific deletion of *Dpp4* in mice to study the role of DPP4 in both normal hematopoiesis and AML development (Figure S4A).[20] The *Dpp4* $^{fl/fl}$: *Vav-Cre*$^+$ (Tm1d or *DPP4*$^{-/-}$) mice displayed an apparently normal phenotype including a normal lifespan when compared with the control *Dpp4* $^{fl/fl}$: *Vav-Cre*$^-$ ($DPP4^{+/+}$) mice. The complete blood count (CBC) of *DPP4*$^{-/-}$ mice is comparable to that of *DPP4*$^{+/+}$ mice (Figure S4B). Furthermore, *DPP4*$^{-/-}$ mice have normal frequency and numbers of HSPC (total of longterm HSCs, short-term HSCs, and multiple potential progenitors) and downstream progenitor cells (including common myeloid progenitors [CMPs], granulocyte-macrophage progenitors [GMPs], and common lymphoid progenitors [CLPs]) in the BM and regular cell-cycle activity of HSCs (Figures S4C-S4F). Consistent with DPP4 inhibition in normal BM cells (Figure 2D), DPP4-deficient BM cells have equal CFU-forming ability as wild-type (WT) cells (Figure S4G). *DPP4*$^{-/-}$ HSCs have higher engraftment ability with no biased lineage reconstitution (Figures S4H and S4I), which is consistent with findings in the DPP4 global knockout mouse model.[21,22]

DPP4 supports AML development in two mouse AML models

Utilizing the *DPP4*$^{-/-}$ and *DPP4*$^{+/+}$ mice generated above with normal hematopoiesis, we retrovirally transduced BM HSPCs derived from these mice with two oncogenes, namely MLL-AF9[16,17] and AML1-ETO9a[23] separately, to generate two AML models to study the role of DPP4 in leukemia development. The efficiency of retrovirus transduction in *DPP4*$^{+/+}$, *DPP4*$^{+/-}$, and *DPP4*$^{-/-}$ HSPCs is comparable as shown in Figure 4A (23% vs. 21% vs. 22%). Intriguingly, MLL-AF9 transformation can greatly raise the level of DPP4 in *DPP4*$^{+/+}$ cells (Figure 4A). The recipient mice transplanted with MLL-AF9-transduced *DPP4*$^{-/-}$ AML cells (henceforth called *DPP4*$^{-/-}$ AML mice) develop leukemia much more slowly than mice transplanted with *DPP4*$^{+/-}$ (heterozygous) and *DPP4*$^{+/+}$ AML cells (on average, *DPP4*$^{-/-}$ AML mice survive >300 days vs. *DPP4*$^{+/-}$ AML mice survive 69.4 days vs. *DPP4*$^{+/+}$ AML mice survive only 40.7 days) in primary transplantation (Figure 4B). Dose dependence of AML development on DPP4 is also evident from the counts of AML cells in PB and DPP4 enzyme activity at 4 weeks post-transplantation (Figures 4C and 4D). Serial tracking of the proportion of YFP^+ AML cells in the PB of *DPP4*$^{-/-}$ AML mice revealed the significantly slow time course of AML development compared with the *DPP4*$^{+/+}$ AML mice at 3 weeks post-transplantation (2.1% vs. 7.6%) that reached relative maximum numbers at 6 weeks post-transplantation (29.4% vs. 88.3%), which then gradually decreased and remained at very low levels (1%–6%, in 8 to 24 week period) (Figure 4E). No comparison was possible after 6 weeks since *DPP4*$^{+/+}$ AML mice were

moribund and euthanized. Similar to PB, the counts and infiltration of *DPP4*$^{-/-}$ AML cells are substantially lower in the various hematopoietic organs compared with those of *DPP4*$^{+/+}$ AML cells at 6 weeks post-transplantation (Figure 4F), which is likely responsible for the significantly smaller size of spleen and liver (Figures 4G and 4H) and less infiltration of AML cells in the hematopoietic organs in recipient mice (Figure 4I). Similar results for survival and engraftment were obtained in another widely used mouse AML model utilizing AML1-ETO9a-transformed AML cells (Figures 4J, 4K, and S5).[5,23] Together, our data indicate that DPP4 plays an essential role in the development of AML.

DPP4 is required for the stemness/activity and survival of AML cells

To further understand the mechanisms underlying dependence of AML development on DPP4, we first measured LSC markers in the BM of the MLL-AF9 mouse model. Surprisingly, at 6 weeks post-transplantation, there were considerably more L-GMP cells in the BM of *DPP4*$^{-/-}$ AML mice compared with *DPP4*$^{+/+}$ AML mice (2.51-fold increase; Figures 5A and 5B),[17] despite the fact that this difference is not immediately apparent at the transformation stage (Figures S6A and S6B). Furthermore, the LSC-harboring population (YFP^{+}Mac1^{+}Kit^{+}) also increased in the BM of *DPP4*$^{-/-}$ AML mice compared with *DPP4*$^{+/+}$ AML mice (2.1-fold; Figures 5C, S6C, and S6D).[5,16] Next, to understand why DPP4 deletion enhanced the number of phenotypic LSCs while preventing AML development, we relied on functional measures to evaluate the activity of LSCs using serial CFU replating and secondary transplantation assays. We observed dramatic reduction in self-renewal of AML-SCs as indicated by stepwise reduction in the activity of *DPP4*$^{-/-}$ AML-SCs in CFU-forming ability of ~50%, ~60%, and ~65% upon serial plating (Figure 5D). Moreover, secondary AML transplantation resulted in much more delayed AML development in *DPP4*$^{-/-}$ AML mice *in vivo* (Figures 5E-5G vs. Figure 4C). Thus, AML-SC activity in *DPP4*$^{-/-}$ AML mice was greatly lowered compared with *DPP4*$^{+/+}$ AML mice. To quantify how DPP4 deficiency affects the AML-SC frequency, we performed transplantations with limiting dilutions of sorted YFP^{+} *DPP4*$^{+/+}$ and *DPP4*$^{-/-}$ MLL-AF9 BM cells that were collected from primary recipients. Figure 5H depicts the progression of leukemia as evaluated by the survival ratio and latency days. Strikingly, the frequency of functional AML-SCs in the *DPP4*$^{-/-}$ primary MLL-AF9 AML model was only 1/675 (= 161/108,740) of that in *DPP4*$^{+/+}$ primary AML mice. Together, these results indicate that DPP4 is required for the stemness of AML cells.

In addition to the role of DPP4 in supporting LSC activity, we examined the mechanisms for substantial reduction of leukemia cells in the PB of *DPP4*$^{-/-}$ AML mice at 6 weeks post-transplantation (Figure 4E) and found that DPP4 deficiency significantly increased apoptosis in the PB of *DPP4*$^{-/-}$ AML mice, (Figures 5J and 5K), which is consistent with our observation in hAML cells treated with DPP4 inhibitors and DPP4 targeting shRNA (Figures 3G and 3N). Serial tracking of AML cell engraftment in *DPP4*$^{-/-}$ AML mice revealed a dramatic reduction in *DPP4*$^{-/-}$ AML cells in all hematopoietic organs from 13 through 50 weeks post-transplantation (Figures 5L, S6E, and S6F). Specifically, BM tracking showed that *DPP4*$^{-/-}$ AML cells were greatly reduced due to apoptosis from 49.3% (apoptotic ratio: 17.3%) at 13 weeks to 12.3% (apoptotic ratio: 3.1%) at 24 weeks and 2.2% (apoptotic ratio: 2.6%) at 50 weeks post-transplantation (Figures 5L and 5M),

which is likely responsible for the substantial reduction of leukemia cells in *DPP4*$^{-/-}$ AML mice during this AML-suppression stage. Consistent with these findings, normal trilineage hematopoiesis was present in the BM of *DPP4*$^{-/-}$ AML mice at 50 weeks post-transplantation, while *DPP4*$^{+/+}$ AML mice at 4 weeks post-transplantation had the marrow largely replaced by immature blasts with large irregular nuclei (Figures 5N and S6G). These data support the notion that DPP4 deletion may suppress/reverse AML development, resulting in AML remission.

NF-κB activation mediates DPP4-initiated intracellular effects on AML-SCs

To determine the mechanisms by which DPP4 regulates the activity and survival of AML cells, we analyzed the genome-wide transcriptome change in *DPP4*$^{+/+}$ vs. *DPP4*$^{-/-}$ MLL-AF9 AML cells. We found that *DPP4*$^{+/+}$ AML cells had much greater expression of genes associated with AML-SC self-renewal and maintenance (Figures 6A and 6B). Quantitative PCR analysis demonstrated significant downregulation of several self-renewal associated genes, such as Hox genes, in MLL-AF9 AML cells, which corroborated with the deep sequencing results (Figure 6C). Reintroduction of DPP4 into *DPP4*$^{-/-}$ AML cells enhanced the level of the self-renewal associated genes (Figure S7A). Importantly, expression of the same self-renewal-associated genes was not different between *DPP4*$^{+/+}$ vs. *DPP4*$^{-/-}$ normal HSPCs (Figure S7B). Gene set enrichment analysis (GSEA) on RNA sequencing (RNA-seq) data revealed that nuclear factor κB (NF-κB) is the most suppressed transcriptional signature in *DPP4*$^{-/-}$ AML cells (normalized enrichment score [NES] = 2.2) compared with *DPP4*$^{+/+}$ AML cells (Figure 6D). To assess the signature of NF-κB inactivation in *DPP4*$^{-/-}$ AML cells, we determined the activation of the signaling intermediates of NF-κB, IκB, and p65 and observed that the phosphorylation of IkB and p65 is dramatically lower in *DPP4*$^{-/-}$ AML cells compared with *DPP4*$^{+/+}$ AML cells. Interestingly, *DPP4*$^{-/-}$ AML cells had higher caspase 3 activity (cleaved caspase 3), which is consistent with our data in hAML, demonstrating that either DPP4 inhibition or deletion can lead to apoptosis in AML cells. In further support of the dependence of DPP4 signaling on NF-κB, other signaling pathways such as pP38MAPK or AKT were not affected (Figure 6E). Importantly, we validated these findings in THP1 AML cells and hAML samples either with shRNA knockdown or linagliptin treatment and observed downregulation of NF-κB intermediates (Figures 6F-6H).

Src is essential to the regulation by DPP4-NF-κB axis of AML development

To understand the molecular mechanism by which DPP4 regulates NF-κB activation, we searched for putative binding partners of DPP4. Among them, the cellular tyrosine kinase Src (c-Src) is an intracellular protein that is a known regulator of AML development.[24,25] Indeed, immunoprecipitation of DPP4 confirmed DPP4-Src binding *in vitro* (Figure 7A). Deficiency of DPP4 in mouse and human AML cells and hAML samples had a marked reduction in Src activation (Figures 7B-7D). In contrast, the activation of Src, IκB, and p65 in normal BM cells of both *DPP4*$^{+/+}$ and *DPP4*$^{-/-}$ mice was low but equal (Figure 7E), suggesting that deletion of DPP4 does not affect Src-NF-κB signaling in normal hematopoiesis. To further test whether DPP4-dependent stemness of AML cells is mediated by Src, we performed CFU assays with *DPP4*$^{+/+}$ and *DPP4*$^{-/-}$ AML cells in the presence of Src family kinase (SFK)-specific inhibitor saracatinib (5 μM). We observed that saracatinib significantly reduces the CFU ability of *DPP4*$^{+/+}$ AML cells but not *DPP4*$^{-/-}$ AML cells

(Figure 7F). To further determine whether Src is essential for DPP4-mediated effects in AML cells, we introduced retroviruses encoding *src* into *DPP4*$^{-/-}$ AML cells. The ectopic expression of Src was capable of reversing the inhibitory phenotype of *DPP4*$^{-/-}$ AML cells to the same level as *DPP4*$^{+/+}$ AML cells in transplantation and CFU assays (Figures 7F-7I). Moreover, the rescue assay samples showed that ectopically expressed Src could activate NF-κB signaling and inhibit caspase signaling, as well as improve the transcriptional level of LSC self-renewal associated genes in *DPP4*$^{-/-}$ AML cells (Figures 7J and 7K). These results demonstrate that DPP4-mediated promotion of AML cell stemness, growth, and NF-κB signaling activation are Src dependent.

DISCUSSION

Currently, the mainstay of AML treatment involves induction chemotherapy followed by consolidation. For AML with high-risk characteristics such as FLT3-ITD mutations or a monosomal karyotype,[26] alloSCT is often the only curative approach. Chemotherapy and alloSCT are highly toxic due to indiscriminate inhibition of a plethora of cellular processes, the so-called off-target effects, which manifest as severe myelosuppression; gastrointestinal symptoms such as vomiting and diarrhea due to effects on dividing cells; infections; bleeding; and graft versus host disease.[1,27] This study identified cell surface protein DPP4 inhibition as a potential treatment for AML. DPP4 inhibitors have been successfully used in the treatment of T2DM for ~15 years and are well tolerated with minimal ADEs such as upper respiratory tract infections, headache, and bloating. Importantly, DPP4 inhibition does not cause severe ADEs such as hypoglycemia, gastrointestinal (GI) side effects (due to inhibition of cell division), and BM suppression.[28-33] This study further validated that DPP4 inhibitors do not affect normal hematopoeisis, which is probably one of the most vexing problems associated with chemotherapy and other novel therapies.

The specificity of DPP4 as a target in AML may be conferred due to the high expression and/or activity of DPP4 and its associated proteins in leukemic cells compared with normal hematopoietic cells. Our studies in mouse AML models showed that DPP4 expression is greatly increased during the HSPC transforming stage (Figures 4A, S2A, and S5), which is consistent with the data that DPP4 expression is significantly higher in CD34^{+} hAML blast cells than CD34^{-} non-blast cells. It was noted that DPP4 expression was significantly higher in a subset of patient-derived hAML samples, implying that DPP4 expression may be associated with specific AML genetic subtypes. FLT3-ITD mutations constitute the largest subgroup of patients with AML (25%) and are associated with a poor prognosis.[34] Significantly, DPP4 is highly expressed in LSCs of patients with AML with FLT3-ITD mutations.[11,13,35] Although FLT3-ITD inhibitors (midostaurin) are approved, they may cause severe ADEs such as fever, respiratory tract infections, and bleeding, all related to BM suppression. Therefore, future studies are needed on the role of DPP4 in the diagnosis and therapy of patients with FLT3-ITD mutant AML.

For decades, the notion of removing the block in LSC differentiation has been explored both to avoid toxicity of chemotherapy to the BM and to guide differentiated cells toward apoptosis in the PB.[36-41] Apart from the success of all-*trans* retinoic acid (ATRA) in acute promyelocytic leukemia (APL), differentiation therapy has not lived up to its promise in

other AML or leukemias, either due to variable responses or due to the development of differentiation syndrome.[40,41] It was intriguing to explore the notion that DPP4 inhibitors may be involved in differentiating leukemia cells since DPP4 has been shown to be involved in cell-cycle arrest and senescence.[42,43] However, when we looked at the cell-cycle stages in our shRNA-mediated knockdown experiments, we did not see evidence of cell-cycle arrest. Moreover, we observed no changes in differentiated populations in the BM of *DPP4*$^{-/-}$ AML mice compared with *DPP4*$^{+/+}$ AML mice, suggesting that DPP4 inhibition does not contribute to AML cell differentiation. Apart from differentiation therapy, other strategies to improve AML treatment include overcoming resistance to chemotherapy by addressing new mutations and/or tumor heterogeneity. Our studies using primary hAML samples further supported the dependence on DPP4 for AML development. This suggests DPP4 deficiency may overcome resistance to therapy in AML. However, true resistance attributable to tumor heterogeneity will require further studies in long-term AML development models.

The role of DPP4 in cancer SCs is not well understood. For example, DPP4 has been identified as a SC marker for both CML and ovarian cancer. While DPP4 is considered as an oncogene in CML, it has been shown to act as a tumor suppressor in ovarian cancer. The differences in downstream mechanisms may be attributed to variations in DPP4 expression levels and the substrates of DPP4 associated with the specific cancer cells. In addition, DPP4 gene expression is regulated via methylation at CpG islands in the 5′ region, which may be altered differently in individual cancers, suggesting that epigenetic regulation may affect the gene function. Furthermore, DPP4 protein expression could be subject to multiple post-translational modifications including glycosylation and acetylation, even sumoylation. In our study, although we observed a paradoxical increase in the phenotypic LSC or LSC-harboring population in *DPP4*$^{-/-}$ AML cells, our data support an increasing dependence of mouse AML-SCs on DPP4 through functional experiments, which manifests as a reduction in engraftment ability after second transplantation and continuous reduction of colony numbers in serial CFU assays. Moreover, the differences in leukemic potential were confirmed by limiting dilution transplantation studies, which revealed that the functional AML-SCs were reduced by 675-fold in the MLL-AF9 model after DPP4 deletion. Taken together, these data suggest that DPP4 confers stemness to the AML cell.

Another interesting finding from our study is that DPP4 inhibition/deletion slowed down growth of AML cells but not normal BM cells. While cell-cycle progression was unchanged in both normal BM and AML cells, apoptosis was prominently affected in the AML cells, and this effect was distinct from Ara-C, which affected both normal BM and AML cells. The increase in apoptosis was observed in both mouse and hAML models and under both DPP4 inhibition and deficient conditions. Increased apoptosis of AML cells and AML-SCs likely resulted in decreased AML cell growth and suppressed AML development that ultimately led to an AML remission-like phenotype on our periodic follow-up studies. DPP4 is a transmembrane protein with a short 6 amino acid sequence with a Src binding motif. We confirmed binding of DPP4 to Src and observed a reduction in phosphorylation and activation of Src-NF-κB signaling with DPP4 deletion in both mouse and hAML, which resulted in improved survival of DPP4$^{-/-}$ AML cells transplanted mice. The dependence on Src for AML growth and survival is consistent with recent findings that the inhibitors of SFK suppress AML cell growth and AML development.[44,45] Transcriptome analysis and

cell signaling studies identified that DPP4-Src-NF-κB signaling works together to promote the survival and activity of AML cells. Inactivation of NF-κB signaling downstream of Src inactivation is consistent both with increased apoptosis in DPP4$^{-/-}$ AML cells and with reports that NF-κB signaling pathway is involved in AML development.[46-48]

In our study, there was a survival difference in AML mice that received DPP4 inhibitor (linagliptin) vs. those that received DPP4-deleted mouse and primary hAML cells. The difference can be attributed to the different levels of DPP4 enzyme inhibition from these two approaches or the contribution of non-enzymatic activity of DPP4 to AML suppression through signaling. Moreover, as DPP4 is expressed on many cell types including AML cells, each with exposure to different substrates, the effect of DPP4 inhibitors is more complex as it involves the net effect of multiple cells and their functions based on different DPP4 substrates.

In summary, the higher rates of apoptosis and reduced stemness of DPP4-deficient and DPP4-inhibited AML cells led to less AML development. Additionally, both of these factors led to reduced tumor burden in the PB and other organs, which might translate to amelioration of leukostasis, clotting problems, shortness of breath, and stroke in patients with leukemia.[49,50] Therefore, DPP4 inhibition may be a viable strategy for treatment of AML, especially in those patients who are unwilling to take or cannot tolerate conventional therapy.[51-53]

Limitations of the study

Our study has identified DPP4 inhibitors as a novel treatment for AML, which specifically targets AML-SCs and not normal HSCs. Although hematopoietic-cell-specific deletion of DPP4 does not affect normal hematopoiesis, and linagliptin does not affect the CFU ability of HSPCs, we cannot completely exclude the impact of linagliptin on LT-HSC function. Price et al. observed no effects on the normal differentiation into the different leukocyte subsets with sitagliptin treatment for 28 days, which further supports the notion that DPP4 inhibition has minimal effects on hematopoiesis of healthy individuals.[54] We and others[35] have observed that DPP4 expression is high in CD34^{+} hAML, specifically the FLT3-ITD subset of patients with AML. However, we have also observed differential expression of DPP4 on CD34^{+} AML-SCs vs. CD34^{-} AML cells, i.e., some hAML samples that are not CD34^{+} have moderate DPP4 expression; whether DPP4 plays role in CD34^{-} AML cells is unknown. These observations align with the MLL-AF9 oncogene-transformed AML cells, which, clinically, are mostly CD34^{-} AML cells, having significantly higher DPP4 expression, partially indicating that DPP4 plays role in CD34^{-} AML cells as well.

STAR★METHODS

RESOURCE AVAILABILITY

Lead contact—Further information and requests for resources and reagents should be directed to and will be fulfilled by the lead contact, Xunlei Kang(Kangxu@health.missouri.edu).

Materials availability—This study did not generate new unique reagents.

Data and code availability—The TCGA datasets analyzed are available in the UCSC Xena Browser (https://xena.ucsc.edu). The RNA-seq datasets generated in the current study have been deposited in NCBI "SRA database: SRP323430."

EXPERIMENTAL MODEL AND SUBJECT DETAILS

Mice—C57 BL/6, CD45.2, CD45.1 mice were purchased from Charles River, Inc. DPP4 flox/flox mice were obtained by breeding targeted C57Bl/6NTac-DPP4tm1a Wtsi/Ics mice (European Mouse Mutant Cell Repository, EUCOMM) with 129S4/Bl6-Gt(ROSA) 26Sortm2(FLP*)Sor/J (stock #012930, The Jackson Laboratory, Bar Harbor, ME). The offspring were then crossed with Vav-iCre mice (stock #018968, The Jackson Laboratory, Bar Harbor, ME) (de Boer et al., 2003),[56] to obtain DPP4 $^{fl/fl}$;Vav-Cre mice. All mice were cared for in accordance with National Institutes of Health guidelines. No statistical method was used to predetermine the sample size. Mice were randomly assigned to the experiments after genotyping with the same sex, similar age group (6–8 weeks old) and approximately same weight. The investigators were not blinded to the allocation of animals during the experiments and outcome assessment. All procedures were approved in advance by the Institutional Animal Care and Use Committee of the University of Missouri.

Human samples—Primary human AML samples were obtained from the tissue banks at University of Missouri, School of Medicine. Informed consent was obtained under protocols reviewed and approved by the Institutional Review Board at University of Missouri (IRB #2018932) to obtain fresh human peripheral blood samples and primary human AML samples at the Ellis Fischel Cancer Center. Diagnosis of AML was confirmed by a pathologist utilizing BM aspiration and biopsy and Cytochemical and Immunohistochemical tests. Cyotgenetics analysis and Next Generation Sequence were performed on the bone marrow by Mayo Clinic Laboratories-Rochester Main Campus. The blood samples were processed using SepMate™-50 (IVD) (STEMCELL Technology GmbH, Germany) according to the manufacturer's instructions and frozen in FBS with 10% DMSO and stored in liquid nitrogen. Information of patient samples including the age and gender have been listed in Figure S3D.

METHOD DETAILS

Cell culture—293T cells were cultured in Dulbecco's Modified Eagle Medium (DMEM) supplemented with 10% FBS at 37°C in 5% CO2. Primary mouse AML cells were cultured in serum-free StemSpan™ (STEMCELL Technologies, Cambridge MA) supplemented with 50 ng/mL SCF, 10 ng/mL IL-3, 10 ng/mL IL-6 (STEMCELL Technologies, Cambridge MA). Human monocytic AML cells THP-1 (ATCC, TIB-202), macrophage B myelomonocytic leukemia MV4-11 (ATCC, CRL-9591), and histiocytic lymphoma U937 (ATCC, CRL-1593.2)) were cultured in Roswell Park Memorial Institute (RPMI) 1640 supplemented with 10% FBS at 37°C in 5% CO_2 and normal O_2. All cell lines were routinely tested using a mycoplasma contamination kit (R&D Systems, Minneapolis MN).

Compound screen for cell surface protein targets—We selected two compound libraries #HYL026 (Clinical Compound Library, MedChemExpress, Monmouth Junction, NJ) and #HYL022 (FDA-Approved Drug Library, MedChemExpress, Monmouth Junction,

NJ), based on a broad panel of cell surface target proteins. #HYL022 and #HYL026 have been used to identify novel targets (Perez-Gomez et al., Nat Commun. 2018 Dec 10; 9(1):5272, Kunder et al. Cell Chem Biol. 2021 Sep 8; S2451-9456(21)00400-1). We did phenotype-based screening, and this approach allows several drugs to be tested without limiting oneself to any single mechanism of action, thereby resulting in first-in-class drugs. We identified 57 candidate compounds based on three pre-specified criteria 1) Low expression of targets of these compounds improved overall survival of AML patients as documented in The Cancer Genome Atlas (TCGA) (Supplementary 1a). 2) *in silico* analysis of gene expression in AML cells. 3) The availability of genetically modified mice for targets of interest. We also ensured that there was no bias in the form of a specific hypothesis in determining which compound to select. We performed the *in vitro* screenings at a concentration of 10mM, including for linagliptin, a DPP4 inhibitor.

Virus construction and infection—pLentiLoxp3.7 (Addgene, Watertown MA) was used to construct DPP4 shRNA expressing lentiviral vectors. The target sequences for sh*DPP4*-1 and sh*DPP4*-2 were 5′ AATGCCAGGAGGAAGGAATCTTT -3′ and 5′ AACAAGTTGAGTACCTCCTTATT -3′, respectively. For virus packaging, retroviral constructs MSCV-MLL-AF9-IRES- YFP/GFP, Mig-AML1-ETO9a or MSCV-SRC-IRES-GFP, were mixed with PCL-ECO (2:1), and the lentivirus constructs were mixed with pSPAX2 and pMD2.G (4:3:1), followed by transfection into 293T cells using PolyJet (SignaGen Laboratories, Frederick MD). Virus-containing supernatant was collected 48–72 h posttransfection and used for infection as described previously.[5] Briefly, the virus supernatant was collected and filtered through a 0.45-mm filter. Lin^- cells were isolated from the bone marrow of littermate $DPP4^{-/-}$ or $DPP4^{+/+}$ mice pretreated with 5-FU (150 mg/kg). For infection of Lin^- cells from bone marrow (BM), Lin^- cells were suspended in virus supernatant supplemented with 4 μg/mL polybrene at 10^5/mL and placed in six-well plates for spin infection (2000 rpm, 90 min at 32°C).

AML transplantation—For primary transplantation, Infected Lin^- cells (2×10^5) were transplanted into lethally irradiated (1,000 cGy) C57BL/6 mice (6–8 weeks old) by retro-orbital injection. For MLL-AF9 AML model, the engraftment was assessed at 4, 6, 13, 24 and 50 weeks post-transplantation, and for AML1-ETO9a AML model, the engraftment was assessed at 20 weeks post-transplantation. For secondary transplantation, we used FACS to isolate YFP^+ or GFP^+ BM cells from primary recipient mice and transplanted 2,000 cells (MLL-AF9 model) together with 2×10^5 normal BM cells into lethally irradiated recipients and engraftment assessed at 3 weeks post-transplantation.

Human AML xenograft—Xenografts were performed essentially as we described previously.[5] Briefly, adult NSG mice (6-8 weeks old) were sublethally irradiated with 250 cGy total body irradiation before transplantation. shRNA-infected cells were resuspended in 200mL PBS containing 2% FBS at a final concentration of 5×10^5 GFP^+ primary human AML viable cells per mouse for retro-orbital injection.

DPP4 activity assay—Plasma-EDTA, bone marrow extracellular fluid (BMEF), or cell lysates were used for DPP4 activity assay. 20 μL each of plasma-EDTA or BMEF or 100 μg

protein was diluted in DPP4 assay buffer (Tris-HCl [pH 8.0], 150 mM NaCl, and protease inhibitor cocktail [Roche Diagnostics]) in a black 96-well plate to a final volume of 50 μL, and 50 μL of the substrate, 200 mM H-Ala-Pro-AFC (I-1680; Bachem Americas, Torrance CA), was added to each well and the plate incubated for 10 min at room temperature in the dark. Fluorescence was measured with a Synergy Microplate Reader at the excitation wavelength of 405 nm and an emission wavelength of 535 nm. Results are reported as relative light units (RLUs).

Leukemia characterization—We performed the procedure as previously described.[57] After transplantation, we monitored the survival, examined the size and histological properties of BM, spleen, and liver, and analyzed the numbers and infiltration of leukemia cells in PB, BM, spleen, and liver. Complete blood counts in PB were measured using a Hemavet 950FS. We also characterized different populations of leukemia cells using flow cytometry. Leukemia characterization was performed by investigators blinded to the experimental groups. Moribund leukemic mice were euthanized and the time was recorded as the time of death. Mice that died for reasons unrelated to leukemia within 10 d after transplantation were excluded from the data analysis.

Flow cytometry—For flow cytometry analyses of mouse PB, BM, Spleen, and Liver, hematopoietic cells were labeled with the following antibodies from Biolegend (San Diego CA) unless specifically indicated: Anti-CD3e-PE/Cyanine5 (mouse, #100310, 1:200 dilution), Anti-Ly-6G/Ly-6C (Gr-1)-PE/Cyanine5 (mouse, #108410, 1:200 dilution), Anti-CD11b-PE/Cyanine5 (mouse, #101210, 1:200 dilution), Anti-CD45R-PE/Cyanine5 (mouse, #103210, 1:200 dilution), Anti-Ter-119-PE/Cyanine5 (mouse, #116210, 1:200 dilution), Anti-CD117 (c-Kit)-APC (mouse, #105812, 1:200 dilution), Anti-Sca-1-PE-cy7 (mouse, #108114, 1:200 dilution), Anti-CD150-PE (mouse, #115904, 1:200 dilution), Anti-CD48-APC/Cyanine7 (mouse, #103432, 1:200 dilution), Anti-Ki67-FITC (mouse, #652410, 1:200 dilution), Hoechst34580 (#565877, BD Pharmingen), Anti-CD16/32-PE (mouse, #101308, 1:200 dilution), Anti-CD34-FITC (mouse, #11-0341-82, 1:200 dilution eBioscience), Anti-CD127-APC/Cyanine7 (mouse, #135040, 1:200 dilution), Anti-CD135-Brilliant Violet421 (mouse, #135314, 1:200 dilution), Annexin V (#640941, 1:20 dilution), PI (#421301, 1:50). Intracellular staining was performed using the Foxp3/Transcription factor staining set (eBioscience, Grand Island NY) and Fixation/Methanol protocol (eBioscience, Grand Island NY) provided by the manufacturers.

Colony assays—Mouse AML cells were diluted to the indicated concentration in IMDM with 2% FBS and were then seeded into methylcellulose medium M3534 or M3434 or H4436 (STEMCELL Technologies, Cambridge MA) for myeloid colony formation analysis, as previously described.[57]

RNA-seq analysis—RNA obtained from sorted BM AML cells of two $DPP4^{+/+}$ and two $DPP4^{-/-}$ AML cells transplanted mice, was purified with QIAGEN miRNeasy Mini Kit. The sample concentration was determined by Qubit fluorometer (Invitrogen, Waltham MA) using the Qubit HS RNA assay kit, and RNA integrity was assessed using the Fragment Analyzer automated electrophoresis system. Next, poly-A containing mRNA was purified

from total RNA (1mg), RNA was fragmented, double-stranded cDNA was generated from fragmented RNA, and the index-containing adapters were ligated to the ends. Libraries were constructed following the manufacturer's protocol with reagents supplied in Illumina's TruSeq mRNA stranded sample preparation kit. The amplified cDNA constructs were purified by addition of Axyprep Mag PCR Clean-up beads. The final construct of each purified library was evaluated using the Fragment Analyzer automated electrophoresis system, quantified with the Qubit fluorometer using the Qubit HS dsDNA assay kit, and diluted according to Illumina's standard sequencing protocol for sequencing on the NextSeq 500. High-throughput sequencing was performed at the University of Missouri DNA Core Facility.

GSEA—GSEA was used to identify gene sets and pathways associated with gene expression data. The input for GSEA was a list of significantly differentially expressed genes (log2 (fold change) > 2, $p < 0.05$, and RPKM >0.5) between two biological states as determined by edgeR. http://software.broadinstitute.org/gsea/index.jsp. GSEA (version 2.2.0) is an analytic tool for relating gene expression data to gene sets to identify unifying biological themes.[55,58] Leukemia stem cell gene sets were obtained from the indicated publication. Gene heat maps were clustered by hierarchical clustering (https://software.broadinstitute.org/morpheus/).

Western blotting—Cells were lysed in Laemmli sample buffer (Sigma-Aldrich, St. Louis MO) supplemented with protease inhibitor cocktail (Roche Diagnostics, Indianapolis IN). Samples were separated on SDS–PAGE gels (Bio-Rad, Hercules CA) and transferred to nitrocellulose membranes (Bio-Rad, Hercules CA) for protein detection as described. Primary antibodies were obtained from Cell Signaling Technology (Danvers MA): p-IKB (2859s, 1:1000 dilution, p-p65 (3039s, 1:1000 dilution), p-Akt (4046s, 1:2000 dilution), p-38MAPK (4092s, 1:1000 dilution), p-SRC (59548s, 1:1000 dilution), Dpp4 (67138s, 1:1000 dilution). Other antibodies were obtained thus: c-src/src (sc-8056, 1:1000 dilution, Santa Cruz Biotechnologies, Dallas TX), β-actin (sc-47778, 1:2000 dilution, Santa Cruz Biotechnologies, Dallas TX), Flag M2 (F1804, 1:10,000 dilution, Sigma-Aldrich, St. Louis MO), and anti HA (16B12, 1:10,000, Covance, Princeton NJ) as well as horseradish peroxidase (HRP) conjugated secondary antibodies (HAF007, 1:1,000, and HAF005, 1:1,000, R&D system, Minneapolis MN) and chemi-luminescent substrate (Invitrogen, Waltham MA).

Blood glucose measurements—Blood samples were analyzed for glucose (AlphaTRACK, Abbott IL) at time 0 and 240 min following Linagliptin (Boehringer Ingleheim, Ingelheim am Rhein, Germany) administration by oral gavage at a concentration of 1 mg/kg.

Quantitative RT-PCR—RT-PCR was performed on 5 ng total RNA with gene-specific primers (as shown below) and a QIAGEN One Step RT-PCR kit (210210; Qiagen, Germantown MD) according to the manufacturer's protocol. β-actin was used as the reference gene to normalize the relative expression for quantitative RT-PCR analysis. RT-qPCR primers used in this study were as follows: *dpp4*: forward (5′- TAC AAA AGT

GAC ATG CCT CAG TT-3′) and reverse (5′- TGT GTA GAG TAT AGA GGG GCA GA-3′); *β-actin*: forward (5′-GCT CTT TTC CAG CCT TCC TT-3′) and reverse (5′-CTT CTG CAT CCT GTC AGC AA-3′); *hoxa5*: forward (5′- CTC ATT TTG CGG TCG CTA TCC-3′) and reverse (5′- ATC CAT GCC ATT GTA GCC GTA-3′); *hoxa3*: forward (5′- TCA GCG ATC TAC GGT GGC TA′) and reverse (5′- GAG GCA AAG GTG GTT CAC CC-3′); *hoxa7*: forward (5′- GCG CTT TTT AGC AAA TAT ACG GC-3′) and reverse (5′- GGG ATG TTT TGG TCG TAG GAG-3′); *hoxa9*: forward (5′- CCC CGA CTT CAG TCC TTG C-3′) and reverse (5′- CCA GGA GCG CAT ATA CCT GC-3′); *hoxa11*: forward (5′- TCT TCG CGC CCA ATG ACA TAC-3′) and reverse (5′- GGC TCA ATG GCG TAC TCT CT-3′); *Meis1*: forward (5′- TCA GCA AAT CTA ACT GAC CAG C-3′) and reverse (5′- AGC TAC ACT GTT GTC CAA GCC-3′); *Myb*: forward (5′- AAC TCC CAC ACC ATT CAA AC-3′) and reverse (5′- GCC ACA ATT CCA GAT TCA TCC-3′); *Mef2c*: forward (5′- ATC CCG ATG CAG ACG ATT CAG-3′) and reverse (5′- AAC AGC ACA CAA TCT TTG CCT-3′).

Bone marrow histology—A bone marrow biopsy was performed at the indicated time points. The biopsy was decalcified in EDTA, embedded in frozen section compound 22 blue (Leica), sectioned at 4 mm, placed onto coated Superfrost Plus Microscope Slides (Fisher Scientific), and fixed in 4% phosphate-buffered formalin. Fixed slides were then stained with hematoxylin/eosin (Thermo Scientific™ Shandon™ Rapid-Chrome H & E Frozen Section Staining Kit). Images were acquired by BZ-8000 fluorescence microscope with a 20x and 60x objective (resulting in 200X and 600x magnification.)

***In silico* analyses and survival analysis—**Data were obtained from the TCGA AML database (https://tcga-data.nci.nih.gov/tcga/, n = 187), the GSE6891 dataset (http://www.ncbi.nlm.nih.gov/geo/query/acc.cgi?acc=GSE6891, n = 520), and the GSE10358 dataset (n = 91). Expression was normalized to total mRNA. Patients were separated into three groups (low, medium, and high) based on the expression levels of DPP4 to perform Kaplan-Meier survival analysis (GraphPad Prism, version 7.0, GraphPad, San Diego CA).

QUANTIFICATION AND STATISTICAL ANALYSIS

Statistical details for each experiment can be found in the respective figure legends. Statistical analysis was performed using Graphpad Prism version 9.0 (GraphPad, San Diego CA). For comparison of two groups, we used Student's t-test and when comparing 3 or more groups, one-way or two-way ANOVA was used with Fisher's test for post-hoc analyses. The survival rates of the two groups were analyzed using a log–rank test and were considered statistically significant if $p < 0.05$. Analysis of RNAseq was analyzed as described in respective methods. Data with error bars represent means ± standard error of the means (SEM). All the experiments had at least 2–3 independent repeats. Different levels of statistical significance were denoted by p values (*$p < 0.05$, **$p < 0.01$, ***$p < 0.001$).

Supplementary Material

Refer to Web version on PubMed Central for supplementary material.

ACKNOWLEDGMENTS

We thank the National Cancer Institute (R37CA241603 to X.K.), the National Institute of Diabetes and Digestive and Kidney Diseases (K08DK115886 to R.N.), the American Heart Association (19CDA34770036 to X.K.), and the Center of Precision Medicine/Department of Medicine (start-up funds to both X.K. and R.N.) for their support. We also thank Dr. Hong Zheng for her careful review and valuable suggestions. We also thank Dr. Tim Ley for many useful discussions.

REFERENCES

1. Tallman MS, Wang ES, Altman JK, Appelbaum FR, Bhatt VR, Bixby D, Coutre SE, De Lima M, Fathi AT, Fiorella M, et al. (2019). Acute myeloid leukemia, version 3.2019, NCCN clinical practice guidelines in oncology. J. Natl. Compr. Canc. Netw 17, 721–749. 10.6004/jnccn.2019.0028. [PubMed: 31200351]
2. Kumar CC (2011). Genetic abnormalities and challenges in the treatment of acute myeloid leukemia. Genes Cancer 2, 95–107. 10.1177/1947601911408076. [PubMed: 21779483]
3. Sanford D, and Ravandi F (2015). Management of newly diagnosed acute myeloid leukemia in the elderly: current strategies and future directions. Drugs Aging 32, 983–997. 10.1007/s40266-015-0309-2. [PubMed: 26446152]
4. Bausch-Fluck D, Hofmann A, Bock T, Frei AP, Cerciello F, Jacobs A, Moest H, Omasits U, Gundry RL, Yoon C, et al. (2015). A mass spectrometric-derived cell surface protein atlas. PLoS One 10, e0121314. 10.1371/journal.pone.0121314. [PubMed: 25894527]
5. Kang X, Lu Z, Cui C, Deng M, Fan Y, Dong B, Han X, Xie F, Tyner JW, Coligan JE, et al. (2015). The ITIM-containing receptor LAIR1 is essential for acute myeloid leukaemia development. Nat. Cell Biol. 17, 665–677. 10.1038/ncb3158. [PubMed: 25915125]
6. Deng M, Gui X, Kim J, Xie L, Chen W, Li Z, He L, Chen Y, Chen H, Luo W, et al. (2018). LILRB4 signalling in leukaemia cells mediates T cell suppression and tumour infiltration. Nature 562, 605–609. 10.1038/s41586-018-0615-z. [PubMed: 30333625]
7. Hopsu-Havu VK, and Glenner GG (1966). A new dipeptide naphthyla-midase hydrolyzing glycyl-prolyl-beta-naphthylamide. Histochemie 7, 197–201. [PubMed: 5959122]
8. Nistala R, and Savin V (2017). Diabetes, hypertension, and chronic kidney disease progression: role of DPP4. Am. J. Physiol. Renal Physiol 312, F661–f670. 10.1152/ajprenal.00316.2016. [PubMed: 28122713]
9. Christopherson KW 2nd, Hangoc G, and Broxmeyer HE (2002). Cell surface peptidase CD26/dipeptidylpeptidase IV regulates CXCL12/stromal cell-derived factor-1 alpha-mediated chemotaxis of human cord blood CD34+ progenitor cells. J. Immunol 169, 7000–7008. [PubMed: 12471135]
10. Christopherson KW 2nd, Cooper S, and Broxmeyer HE (2003). Cell surface peptidase CD26/DPPIV mediates G-CSF mobilization of mouse progenitor cells. Blood 101, 4680–4686. 10.1182/blood-2002-12-3893. [PubMed: 12576320]
11. Herrmann H, Sadovnik I, Cerny-Reiterer S, Rülicke T, Stefanzl G, Willmann M, Hoermann G, Bilban M, Blatt K, Herndlhofer S, et al. (2014). Dipeptidylpeptidase IV (CD26) defines leukemic stem cells (LSC) in chronic myeloid leukemia. Blood 123, 3951–3962. 10.1182/blood-2013-10-536078. [PubMed: 24778155]
12. Castillo JJ, Mull N, Reagan JL, Nemr S, and Mitri J (2012). Increased incidence of non-Hodgkin lymphoma, leukemia, and myeloma in patients with diabetes mellitus type 2: a meta-analysis of observational studies. Blood 119, 4845–4850. 10.1182/blood-2011-06-362830. [PubMed: 22496152]
13. Blatt K, Menzl I, Eisenwort G, Cerny-Reiterer S, Herrmann H, Herndlhofer S, Stefanzl G, Sadovnik I, Berger D, Keller A, et al. (2018). Phenotyping and target expression Profiling of CD34(+)/CD38(−) and CD34(+)/CD38(+) stem- and progenitor cells in acute lymphoblastic leukemia. Neoplasia 20, 632–642. 10.1016/j.neo.2018.04.004. [PubMed: 29772458]
14. O'Leary HA, Capitano M, Cooper S, Mantel C, Boswell HS, Kapur R, Ramdas B, Chan R, Deng L, Qu CK, and Broxmeyer HE (2017). DPP4 truncated GM-CSF and IL-3 manifest distinct receptor-binding and regulatory functions compared with their full-length forms. Leukemia 31, 2468–2478. 10.1038/leu.2017.98. [PubMed: 28344320]

15. Namburi S, Broxmeyer HE, Hong CS, Whiteside TL, and Boyiadzis M (2021). DPP4(+) exosomes in AML patients' plasma suppress proliferation of hematopoietic progenitor cells. Leukemia 35, 1925–1932. 10.1038/s41375-020-01047-7. [PubMed: 33139859]

16. Somervaille TCP, and Cleary ML (2006). Identification and characterization of leukemia stem cells in murine MLL-AF9 acute myeloid leukemia. Cancer Cell 10, 257–268. 10.1016/j.ccr.2006.08.020. [PubMed: 17045204]

17. Krivtsov AV, Twomey D, Feng Z, Stubbs MC, Wang Y, Faber J, Levine JE, Wang J, Hahn WC, Gilliland DG, et al. (2006). Transformation from committed progenitor to leukaemia stem cell initiated by MLL-AF9. Nature 442, 818–822. 10.1038/nature04980. [PubMed: 16862118]

18. Wiernik PH, Banks PL, Case DC Jr., Arlin ZA, Periman PO, Todd MB, Ritch PS, Enck RE, and Weitberg AB (1992). Cytarabine plus idarubicin or daunorubicin as induction and consolidation therapy for previously untreated adult patients with acute myeloid leukemia. Blood 79, 313–319. [PubMed: 1730080]

19. Robak T, and Wierzbowska A (2009). Current and emerging therapies for acute myeloid leukemia. Clin. Ther 31 Pt 2, 2349–2370. 10.1016/j.clinthera.2009.11.017. [PubMed: 20110045]

20. Skarnes WC, Rosen B, West AP, Koutsourakis M, Bushell W, Iyer V, Mujica AO, Thomas M, Harrow J, Cox T, et al. (2011). A conditional knockout resource for the genome-wide study of mouse gene function. Nature 474, 337–342. 10.1038/nature10163. [PubMed: 21677750]

21. Christopherson KW 2nd, Hangoc G, Mantel CR, and Broxmeyer HE (2004). Modulation of hematopoietic stem cell homing and engraftment by CD26. Science 305, 1000–1003. 10.1126/science.1097071. [PubMed: 15310902]

22. Broxmeyer HE, Hoggatt J, O'Leary HA, Mantel C, Chitteti BR, Cooper S, Messina-Graham S, Hangoc G, Farag S, Rohrabaugh SL, et al. (2012). Dipeptidylpeptidase 4 negatively regulates colony-stimulating factor activity and stress hematopoiesis. Nat. Med 18, 1786–1796. 10.1038/nm.2991. [PubMed: 23160239]

23. Yan M, Kanbe E, Peterson LF, Boyapati A, Miao Y, Wang Y, Chen IM, Chen Z, Rowley JD, Willman CL, and Zhang DE (2006). A previously unidentified alternatively spliced isoform of t(8;21) transcript promotes leukemogenesis. Nat. Med 12, 945–949. 10.1038/nm1443. [PubMed: 16892037]

24. De Grandis M, Bardin F, Fauriat C, Zemmour C, El-Kaoutari A, Sergé A, Granjeaud S, Pouyet L, Montersino C, Chretien AS, et al. (2017). JAM-C identifies src family kinase-activated leukemia-initiating cells and predicts poor prognosis in acute myeloid leukemia. Cancer Res. 77, 6627–6640. 10.1158/0008-5472.CAN-17-1223. [PubMed: 28972073]

25. MacDonald RJ, Bunaciu RP, Ip V, Dai D, Tran D, Varner JD, and Yen A (2018). Src family kinase inhibitor bosutinib enhances retinoic acid-induced differentiation of HL-60 leukemia cells. Leuk. Lymphoma 59, 2941–2951. 10.1080/10428194.2018.1452213. [PubMed: 29569971]

26. Estey EH (2012). How to manage high-risk acute myeloid leukemia. Leukemia 26, 861–869. 10.1038/leu.2011.317. [PubMed: 22116555]

27. Haubner S, Perna F, Köhnke T, Schmidt C, Berman S, Augsberger C, Schnorfeil FM, Krupka C, Lichtenegger FS, Liu X, et al. (2019). Coexpression profile of leukemic stem cell markers for combinatorial targeted therapy in AML. Leukemia 33, 64–74. 10.1038/s41375-018-0180-3. [PubMed: 29946192]

28. (2012). Lingliptin Drug Evaluation and Research Application Number: NDA 201280/S-002 (Clinical Trial).

29. Graefe-Mody U, Retlich S, and Friedrich C (2012). Clinical pharmacokinetics and pharmacodynamics of linagliptin. Clin. Pharmacokinet. 51, 411–427. 10.2165/11630900-000000000-00000. [PubMed: 22568694]

30. Conarello SL, Li Z, Ronan J, Roy RS, Zhu L, Jiang G, Liu F, Woods J, Zycband E, Moller DE, et al. (2003). Mice lacking dipeptidyl peptidase IV are protected against obesity and insulin resistance. Proc. Natl. Acad. Sci. USA 100, 6825–6830. 10.1073/pnas.0631828100. [PubMed: 12748388]

31. Marguet D, Baggio L, Kobayashi T, Bernard AM, Pierres M, Nielsen PF, Ribel U, Watanabe T, Drucker DJ, and Wagtmann N (2000). Enhanced insulin secretion and improved glucose tolerance

in mice lacking CD26. Proc. Natl. Acad. Sci. USA 97, 6874–6879. 10.1073/pnas.120069197. [PubMed: 10823914]

32. Gallwitz B, Rosenstock J, Rauch T, Bhattacharya S, Patel S, von Eynatten M, Dugi KA, and Woerle HJ (2012). 2-year efficacy and safety of linagliptin compared with glimepiride in patients with type 2 diabetes inadequately controlled on metformin: a randomised, double-blind, noninferiority trial. Lancet 380, 475–483. 10.1016/S0140-6736(12)60691-6. [PubMed: 22748821]
33. Scheen AJ (2018). The safety of gliptins : updated data in 2018. Expert Opin. Drug Saf 17, 387–405. 10.1080/14740338.2018.1444027. [PubMed: 29468916]
34. Tao S, Wang C, Chen Y, Deng Y, Song L, Shi Y, Ling L, Ding B, He Z, and Yu L (2019). Prognosis and outcome of patients with acute myeloid leukemia based on FLT3-ITD mutation with or without additional abnormal cytogenetics. Oncol. Lett 18, 6766–6774. 10.3892/ol.2019.11051. [PubMed: 31807186]
35. Herrmann H, Sadovnik I, Eisenwort G, Rülicke T, Blatt K, Herndlhofer S, Willmann M, Stefanzl G, Baumgartner S, Greiner G, et al. (2020). Delineation of target expression profiles in CD34+/CD38− and CD34+/CD38+ stem and progenitor cells in AML and CML. Blood Adv. 4, 5118–5132. 10.1182/bloodadvances.2020001742. [PubMed: 33085758]
36. Riewald M, Chuang T, Neubauer A, Riess H, and Schleef RR (1998). Expression of bomapin, a novel human serpin, in normal/malignant hematopoiesis and in the monocytic cell lines THP-1 and AML-193. Blood 91, 1256–1262. [PubMed: 9454755]
37. Gudas LJ, and Wagner JA (2011). Retinoids regulate stem cell differentiation. J. Cell. Physiol. 226, 322–330. 10.1002/jcp.22417. [PubMed: 20836077]
38. Bots M, Verbrugge I, Martin BP, Salmon JM, Ghisi M, Baker A, Stanley K, Shortt J, Ossenkoppele GJ, Zuber J, et al. (2014). Differentiation therapy for the treatment of t(8;21) acute myeloid leukemia using histone deacetylase inhibitors. Blood 123, 1341–1352. 10.1182/blood-2013-03-488114. [PubMed: 24415537]
39. Germano G, Morello G, Aveic S, Pinazza M, Minuzzo S, Frasson C, Persano L, Bonvini P, Viola G, Bresolin S, et al. (2017). ZNF521 sustains the differentiation block in MLL-rearranged acute myeloid leukemia. Oncotarget 8, 26129–26141. 10.18632/oncotarget.15387. [PubMed: 28412727]
40. Nowak D, Stewart D, and Koeffler HP (2009). Differentiation therapy of leukemia: 3 decades of development. Blood 113, 3655–3665. 10.1182/blood-2009-01-198911. [PubMed: 19221035]
41. Madan V, and Koeffler HP (2021). Differentiation therapy of myeloid leukemia: four decades of development. Haematologica 106, 26–38. 10.3324/haematol.2020.262121. [PubMed: 33054125]
42. Kim KM, Noh JH, Bodogai M, Martindale JL, Yang X, Indig FE, Basu SK, Ohnuma K, Morimoto C, Johnson PF, et al. (2017). Identification of senescent cell surface targetable protein DPP4. Genes Dev. 31, 1529–1534. 10.1101/gad.302570.117. [PubMed: 28877934]
43. Li L, van Breugel PC, Loayza-Puch F, Ugalde AP, Korkmaz G, Messika-Gold N, Han R, Lopes R, Barbera EP, Teunissen H, et al. (2018). LncRNA-OIS1 regulates DPP4 activation to modulate senescence induced by RAS. Nucleic Acids Res. 46, 4213–4227. 10.1093/nar/gky087. [PubMed: 29481642]
44. Weir MC, Shu ST, Patel RK, Hellwig S, Chen L, Tan L, Gray NS, and Smithgall TE (2018). Selective inhibition of the myeloid src-family kinase Fgr potently suppresses AML cell growth in vitro and in vivo. ACS Chem. Biol. 13, 1551–1559. 10.1021/acschembio.8b00154. [PubMed: 29763550]
45. Bilodeau N, Fiset A, Poirier GG, Fortier S, Gingras MC, Lavoie JN, and Faure RL (2006). Insulin-dependent phosphorylation of DPP IV in liver. Evidence for a role of compartmentalized c-Src. FEBS J. 273, 992–1003. 10.1111/j.1742-4658.2006.05125.x. [PubMed: 16478473]
46. Wei TYW, Wu PY, Wu TJ, Hou HA, Chou WC, Teng CLJ, Lin CR, Chen JMM, Lin TY, Su HC, et al. (2017). Aurora A and NF-kappaB survival pathway drive chemoresistance in acute myeloid leukemia via the TRAF-interacting protein TIFA. Cancer Res. 77, 494–508. 10.1158/0008-5472.CAN-16-1004. [PubMed: 28069801]
47. Wang WL, Xu QZ, Mu XH, Wang L, Zhang LY, Xu J, Gao YD, Cheng T, and Yuan WP (2016). [Role of NF-kappaB inhibitor in acute myeloid leukemia]. Zhongguo Shi Yan Xue Ye Xue Za Zhi 24, 1622–1626. 10.7534/j.issn.1009-2137.2016.06.002. [PubMed: 28024466]

48. Bosman MCJ, Schuringa JJ, and Vellenga E (2016). Constitutive NF-kappaB activation in AML: causes and treatment strategies. Crit. Rev. Oncol. Hematol 98, 35–44. 10.1016/j.critrevonc.2015.10.001. [PubMed: 26490297]

49. Cline A, Jajosky R, Shikle J, and Bollag R (2018). Comparing leuka-pheresis protocols for an AML patient with symptomatic leukostasis. J. Clin. Apher 33, 396–400. 10.1002/jca.21588. [PubMed: 28940295]

50. Del Prete C, Kim T, Lansigan F, Shatzel J, and Friedman H (2018). The epidemiology and clinical associations of stroke in patients with acute myeloid leukemia: a review of 10,972 admissions from the 2012 national inpatient sample. Clin. Lymphoma Myeloma Leuk 18, 74–77.e1. 10.1016/j.clml.2017.09.008. [PubMed: 29097159]

51. Thol F, Schlenk RF, Heuser M, and Ganser A (2015). How I treat refractory and early relapsed acute myeloid leukemia. Blood 126, 319–327. 10.1182/blood-2014-10-551911. [PubMed: 25852056]

52. Sasine JP, and Schiller GJ (2015). Emerging strategies for high-risk and relapsed/refractory acute myeloid leukemia: novel agents and approaches currently in clinical trials. Blood Rev. 29, 1–9. 10.1016/j.blre.2014.07.002. [PubMed: 25441922]

53. Nazha A, and Ravandi F (2014). Acute myeloid leukemia in the elderly: do we know who should be treated and how? Leuk. Lymphoma 55, 979–987. 10.3109/10428194.2013.828348. [PubMed: 23885839]

54. Price JD, Linder G, Li WP, Zimmermann B, Rother KI, Malek R, Alattar M, and Tarbell KV (2013). Effects of short-term sitagliptin treatment on immune parameters in healthy individuals, a randomized placebo-controlled study. Clin. Exp. Immunol 174, 120–128. 10.1111/cei.12144. [PubMed: 23711188]

55. Mootha VK, Lindgren CM, Eriksson KF, Subramanian A, Sihag S, Lehar J, Puigserver P, Carlsson E, Ridderstråle M, Laurila E, et al. (2003). PGC-1alpha-responsive genes involved in oxidative phosphorylation are coordinately downregulated in human diabetes. Nat. Genet 34, 267–273. 10.1038/ng1180. [PubMed: 12808457]

56. de Boer J, Williams A, Skavdis G, Harker N, Coles M, Tolaini M, Norton T, Williams K, Roderick K, Potocnik AJ, and Kioussis D (2003). Transgenic mice with hematopoietic and lymphoid specific expression of Cre. Eur. J. Immunol 33, 314–325. 10.1002/immu.200310005. [PubMed: 12548562]

57. Kang X, Cui C, Wang C, Wu G, Chen H, Lu Z, Chen X, Wang L, Huang J, Geng H, et al. (2018). CAMKs support development of acute myeloid leukemia. J. Hematol. Oncol 11, 30. 10.1186/s13045-018-0574-8. [PubMed: 29482582]

58. Subramanian A, Tamayo P, Mootha VK, Mukherjee S, Ebert BL, Gillette MA, Paulovich A, Pomeroy SL, Golub TR, Lander ES, and Mesirov JP (2005). Gene set enrichment analysis: a knowledge- based approach for interpreting genome-wide expression profiles. Proc. Natl. Acad. Sci. USA 102, 15545–15550. 10.1073/pnas.0506580102. [PubMed: 16199517]

Highlights

- AML cell survival depends on DPP4-mediated upregulation of Src-NF-κB axis
- DPP4 deficiency renders AML cells susceptible to apoptosis while sparing normal HSCs
- DPP4 confers stemness to AML cells
- Currently available DPP4 inhibitors could be added to therapeutic regimen in AML

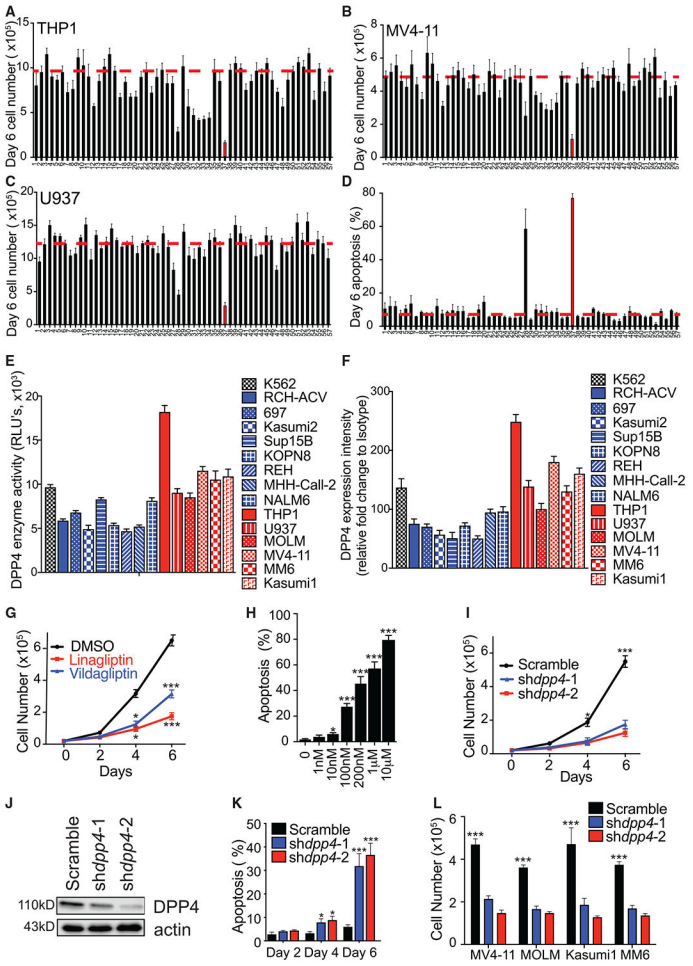

Figure 1. Growth of AML cells is dependent on DPP4

(A–C) Cell numbers of THP1 (A), MV4-11 (B), and U937 (C) on day 6 of treatment with 57 select compounds (details in Figure S1A), each at a concentration of 10 μM (n = 3 wells). The dotted red line indicates the cell number with DMSO treatment (control), and the red bar indicates treatment with compound 37 (linagliptin, DPP4 inhibitor).

(D) Proportion of apoptotic THP1 cells on day 6 of treatment with 57 select compounds (n = 3 wells).

(E) The DPP4 enzyme activity of 1×10^6 human leukemic cells was measured by a fluorescence assay. Results are reported as relative light units (RLUs) (n = 3 wells).

(F) Human leukemic cells' medium fluorescent intensity (MFI) of DPP4 relative to isotype as determined by flow cytometry (n = 3 wells).

(G) DPP4 inhibitors (linagliptin 200 nM, vildagliptin 300 nM) suppress the growth of THP1 cells (n = 3 wells).

(H) Apoptosis in linagliptin-treated THP1 cells at indicated concentrations (n = 3 wells).

(I–K) Treatment with shRNA-targeting DPP4 inhibits the growth of THP1 cells. Two different DPP4-targeting shRNAs inhibit the growth of THP1 cells (I, n = 3 wells). Knockdown of DPP4 in THP1 cells was evaluated by western blot (WB) (J). Proportion of apoptotic cells was measured on the indicated days (K, n = 3 samples). (L) DPP4

knockdown inhibited the growth of MV4-11, MOLM, Kasumi1, and MM6 cells as measured on day 6 (n = 3 wells).

Error bars, SEM. *p < 0.05, ***p < 0.001. Data were analyzed using two-tailed Student's t test; when comparing 3 or more groups, one-way or two-way ANOVA was used with Fisher's test for post-hoc analyses.

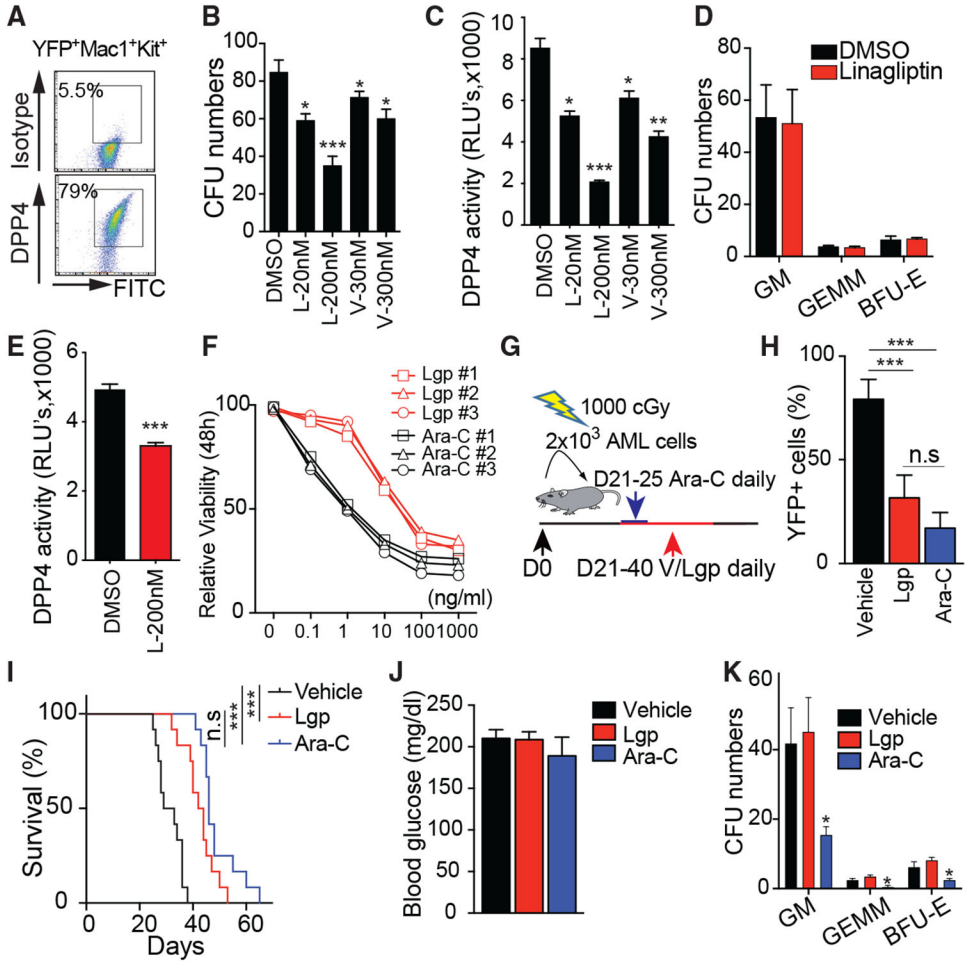

Figure 2. DPP4 inhibitors suppress AML development, not the activity of HSPCs

(A) Dot plots showing DPP4 expression on *DPP4*$^{+/+}$YFP^{+}Mac-1^{+}Kit^{+}AML cells (4 weeks after transplantation) as determined by flow cytometry.

(B and C) Comparative efficacies of two different DPP4 inhibitors at indicated concentrations in suppression of mouse MLL-AF9 cell CFU numbers (B, 2,000 cells/well, n = 3 wells) and DPP4 enzyme activity of 1 × 10^6 cells (C, n = 3 repeats). L, linagliptin; V, vildagliptin.

(D) The effect of linagliptin treatment (200 nM) on normal mouse BM cell CFU-forming ability (10,000 cells/well n = 3 wells).

(E) DPP4 enzyme activity inhibition by linagliptin treatment (200 nM) on 1 × 10^6 mouse BM HSPCs (n = 3 wells).

(F) Comparison of the efficacy of linagliptin (Lgp; at 0.21, 2.1, 21, 210, and 2,100 nM, respectively) and Ara-C (at 0.41, 4.1, 41, 410, and 4,100 nM, respectively) chemotherapy *in vitro*, corresponding to 0.1, 1.0, 10, 100, and 1,000 ng/mL of each (n = 3, AML cells were obtained from 3 MLL-AF9 AML cell-transplanted mice).

(G) Schematic representation of *in vivo* treatment protocol. The regimen consisted of daily intraperitoneal injections of cytarabine (Ara-C, 100 mg/kg/day over 5 days) or vehicle (V)/Lgp (1 mg/kg/day over 20 days). D, day.

(H) The percentage of YFP^+ AML cells in PB of V−, Lgp−, or Ara-C-treated mice at 30 days post-transplantation (n = 5 mice).
(I) Survival curve of MLL-AF9 AML mice treated with V (n = 20 mice), Lgp (n = 12 mice), or Ara-C (n = 12 mice). p values were derived from a log rank test.
(J) Fasting glucose levels in V−, Lgp−, or Ara-C-treated mice at 30 days post-transplantation (n = 5 mice).
(K) Comparison of CFU-forming ability of non-AML cells (YFP^- BM cells, 10,000 cells per well, n = 3 wells) obtained from V−, Lg−, or Ara-C-treated mice at 30 days post-transplantation.
Error bars, SEM. *p < 0.05, ***p < 0.001. Data were analyzed using two-tailed Student's t test; when comparing 3 or more groups, one-way or two-way ANOVA was used with Fisher's test for post-hoc analyses.

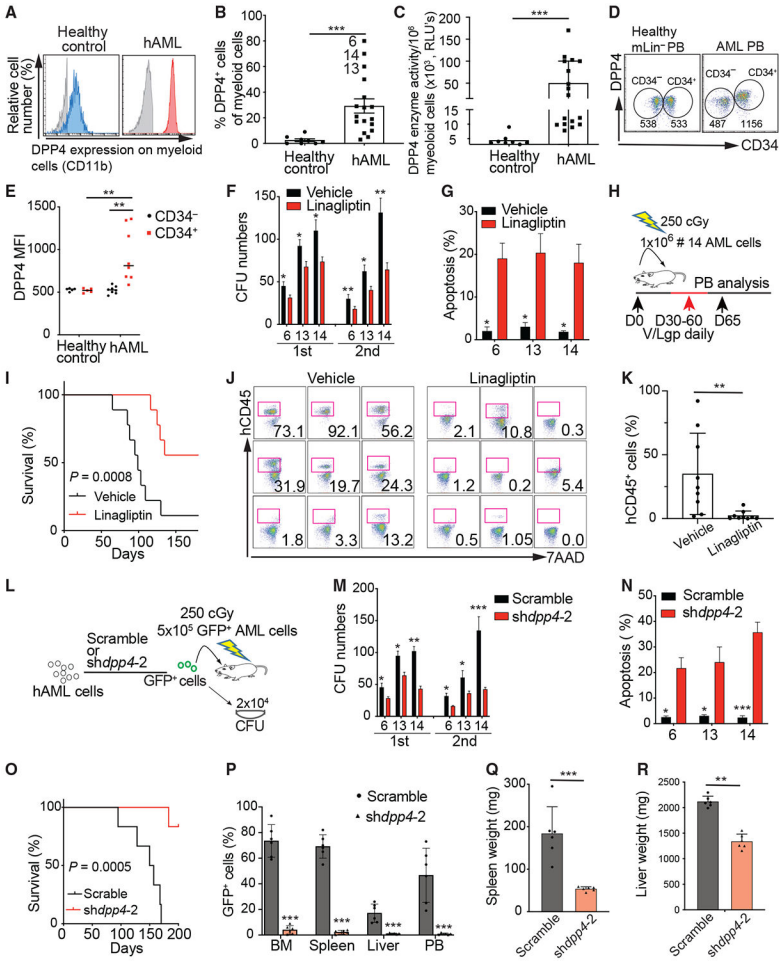

Figure 3. Human AML growth is dependent on increased expression and activity of DPP4

(A) Histograms depicting DPP4 expression in the PB of human healthy controls and patients with AML: red indicates a positive staining reaction, blue indicates a negative staining reaction, and the isotype-matched control antibody is shown in gray.

(B and C) Proportion of DPP4$^+$ myeloid cells (B) or DPP4 enzyme activity (C) in PB of patients with AML (n = 17) and healthy controls (n = 8).

(D) Representative flow cytometry plots to measure cell surface expression of DPP4; the numbers indicate the MFI value of gated cells. mlin$^-$ indicates mobilized PB lineage$^-$ cells.

(E) Summary of DPP4 expression in CD34$^+$ and CD34$^-$ populations of human healthy mobilized PB lineage$^-$ cells (n = 5 samples) and patient with AML PB cells (n = 8 samples).

(F) Lgp suppressed DPP4$^+$ AML cell CFU-forming ability in serial plating of AML patients #6, #13, and #14 (10,000 cells per well, n = 3 wells). In addition, 10,000 live cells from the first CFUs were used to perform the second CFU assay to test the stemness of AML cells.

(G) Lgp treatment increased the proportion of apoptotic AML cells after primary CFU assay (n = 3 wells), Annexin V was used (100,000 cells) to measure apoptosis on the cells from the first CFU assay.

(H) Schematic representation of the treatment protocol in hAML cell (sample #14)-transplanted NSG mice, which consisted of daily intraperitoneal injections of V or Lgp (1 mg/kg/day over 30 days). D, day.

(I) Survival curve of hAML cell-transplanted NSG mice treated with V or Lgp (n = 9 mice). p values were derived from a log rank test.
(J and K) Flow cytometry analysis (J) and histograms (K) of PB cells on day 65 showed Lgp treatment greatly reduced AML cell engraftment in NSG mice (n = 9 mice in each group). The number indicated the percentage of gated human $CD45^+$ AML cells with 7AAD staining to exclude the dead cells.
(L) Schematic representation of the experiment design used to knock down *dpp4* in hAML cells (sample #14) and then perform CFU and xenograft assays.
(M) Comparison of CFU-forming ability in serial plating after DPP4 knockdown in hAML cells (10,000 cells per well, n = 3 wells).
(N) DPP4 knockdown increased the proportion of apoptotic AML cells in primary CFU assay (n = 3 wells).
(O) Survival curve of hAML cell-transplanted NSG mice infected with scramble or *shdpp4*-2 virus (n = 6 mice). p values were derived from a log rank test.
(P) Summary of the proportions of GFP^+ cells in BM, spleen, liver, and PB at day 150 after transplantation or when they were sacrificed (n = 6 mice).
(Q and R) Comparison of the weight of spleens (Q) and livers (R) of the mice transplanted with hAML cells expressing shRNA-targeting *dpp4* or scramble control (n = 6 mice).
Error bars, SEM. *p < 0.05, **p < 0.01, ***p < 0.001. Data were analyzed using two-tailed Student's t test; when comparing 3 or more groups, one-way or two-way ANOVA was used with Fisher's test for post-hoc analyses.

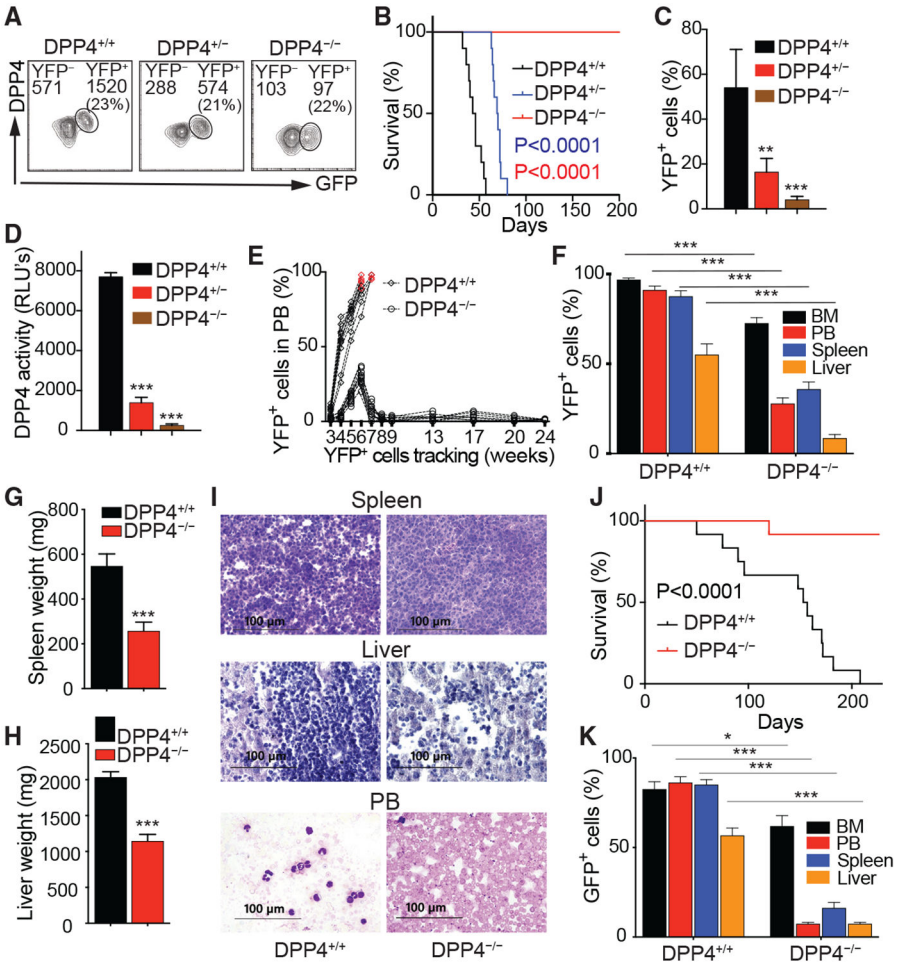

Figure 4. DPP4 supports AML development in two mouse AML models

(A) Contour plots showing the infection efficiency (numbers in the parenthesis indicate the proportions of YFP$^+$ cells) of *DPP4*$^{+/+}$, *DPP4*$^{+/-}$, or *DPP4*$^{-/-}$ HSPCs transduced with MLL-AF9-IRES-YFP retrovirus 40 h after infection. DPP4 MFIs of YFP$^+$ and YFP$^-$ populations have been indicated.

(B) Survival curve of mice receiving MLL-AF9-infected *DPP4*$^{+/+}$, *DPP4*$^{+/-}$, or *DPP4*$^{-/-}$ HSPCs (n = 10 mice).

(C) The proportions of YFP$^+$ AML cells in PB of mice transplanted with *DPP4*$^{+/+}$, *DPP4*$^{+/-}$, or *DPP4*$^{-/-}$ AML cells at 4 weeks post-transplantation (n = 10 mice).

(D) The DPP4 enzyme activity of 1 × 10^6 AML cells were measured by fluorescence assay (n = 3 mice).

(E) Summary of the proportions of YFP$^+$ *DPP4*$^{+/+}$ and *DPP4*$^{-/-}$ MLL-AF9 leukemia cells in PB of primary transplanted mice over time (n = 10 mice). Red dots indicate the moribund stage of the mice, which were sacrificed at that time point.

(F–H) Comparison of the proportions of YFP$^+$ AML cells in BM, PB, spleen, and liver (F), the spleen weight (G), and liver weight (H) of mice transplanted with *DPP4*$^{+/+}$ MLL-AF9 cells and those with *DPP4*$^{-/-}$ MLL-AF9 cells at 6 weeks post-transplantation (n = 3 mice).

(I) Histological analysis of AML infiltration in the spleen, liver, and PB of mice at 6 weeks posttransplantation (hematoxylin and eosin staining for spleen and liver, HEMA 3 staining

for PB samples). Shown are representative images from at least three similar images. Scale bar is 100 μM.

(J) Survival curves of mice receiving AML1-ETO9a-infected *DPP4*$^{+/+}$ or *DPP4*$^{-/-}$ HSPCs (n = 12 mice; $p < 0.0001$, log rank test).

(K) Proportions of AML1-ETO9a GFP^{+} leukemia cells in BM at 20 weeks after transplantation (n = 6 mice).

Error bars, SEM. *$p < 0.05$, **$p < 0.01$, ***$p < 0.001$. Data were analyzed using two-tailed Student's t test; when comparing 3 or more groups, one-way or two-way ANOVA was used with Fisher's test for post-hoc analyses, except that the p values of (B) and (J) were derived from log rank tests.

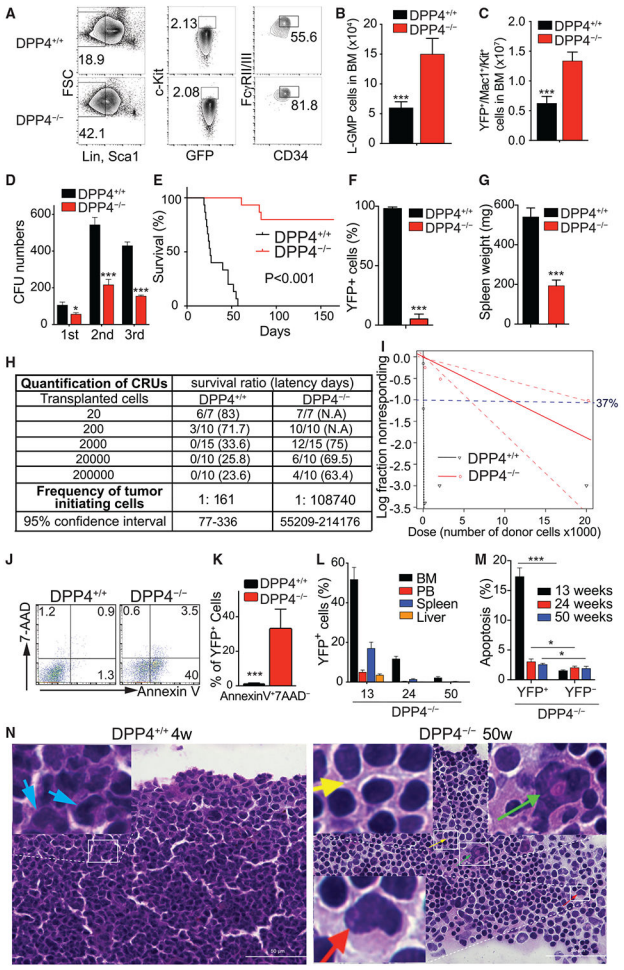

Figure 5. DPP4 deletion leads to an AML remission-like state via increase in apoptosis of AML cells and reduction in the activity of AML-SCs

(A) Immunophenotypic analysis of myeloid progenitors from the BM of *DPP4*$^{+/+}$ and *DPP4*$^{-/-}$ MLL-AF9 AML mice at 6 weeks post-transplantation to identify the L-GMP population.

(B) Summary of absolute numbers of L-GMP in the BM of *DPP4*$^{+/+}$ and *DPP4*$^{-/-}$ MLL-AF9 AML mice at 6 weeks post-transplantation (n = 5 mice).

(C) Summary of absolute numbers of YFP^{+} Mac1^{+} Kit^{+} AML cells in the BM of *DPP4*$^{+/+}$ and *DPP4*$^{-/-}$ MLL-AF9 AML mice at 6 weeks post-transplantation (n = 5 mice).

(D) Comparison of CFU capability of *DPP4*$^{+/+}$ and *DPP4*$^{-/-}$ MLL-AF9 AML cells during serial re-plating (2,000 cells/well, n = 3 wells).

(E) Survival curve of secondary transplanted mice receiving 2,000 *DPP4*$^{+/+}$ or *DPP4*$^{-/-}$ AML cells (n = 10 mice; $p < 0.001$, log rank test).

(F) The proportion of YFP^{+} AML cells in PB of mice secondary transplanted with *DPP4*$^{+/+}$ or *DPP4*$^{-/-}$ AML cells at 3 weeks post-transplantation (n = 10 mice).

(G) Comparison of the spleen weight of mice secondary transplanted with *DPP4*$^{+/+}$ MLL-AF9 cells and those with *DPP4*$^{-/-}$ AML cells at 3 weeks post-transplantation (n = 3 mice).

(H and I) Limiting dilution assays comparing the frequencies of AML stem cells in *DPP4*$^{+/+}$ and *DPP4*$^{-/-}$ MLL-AF9^{+} AML. The indicated YFP^{+} *DPP4*$^{+/+}$ and *DPP4*$^{-/-}$ MLL-AF9^{+}

BM cells that were collected from primary recipients were co-transplanted with 2 × 105 BM competitor cells into lethally irradiated recipients. Mice were followed for 6 months, and at the end of the follow-up period, flow cytometry analysis confirmed the absence of YFP^+ donor leukemia cells in BM and subclinical disease in surviving mice. The competitive repopulating units (CRUs) were calculated by L-Calc software (v.1.1; StemCell Technologies).

(J and K) Representative image and plots of flow cytometry analysis of apoptosis in mouse YFP^+ AML cells from PB at 6 weeks post-transplantation; apoptosis was detected as Annexin $V^+/PE^+/7\text{-}AAD^-$ staining (n = 5 mice).

(L) Comparison of the proportions of YFP^+ AML cells in BM, PB, spleen, and liver of mice transplanted with *DPP4*$^{-/-}$ AML cells at 13, 24, and 50 weeks posttransplantation (n = 5 mice).

(M) Flow cytometry analysis of apoptosis in mouse MLL-AF9 YFP^+ (AML) cells and YFP^- (normal) cells of the BM of *DPP4*$^{-/-}$ MLL-AF9 at the indicated time points. Apoptosis was detected as Annexin V^+ $7\text{-}AAD^-$ staining (n = 5 mice).

(N) Histological analysis of AML infiltration in the BM of mice transplanted with *DPP4*$^{+/+}$ AML cells (4 weeks post-transplantation) or *DPP4*$^{-/-}$ AML cells (50 weeks post-transplantation). Hematoxylin and eosin (H&E) stain, original magnification, ×600. Scale bar is 50 μM. The dashed lines outline a sampling of immature blasts (blue arrow), and trilineage cells, erythroid (yellow arow), megakaryocyte (green arrow), and mature myeloid (red arrow).

Error bars, SEM. *$p < 0.05$, ***$p < 0.001$. Data were analyzed using two-tailed Student's t test; when comparing 3 or more groups, one-way or two-way ANOVA was used with Fisher's test for post-hoc analyses, except that the p value of (E) was derived from log rank tests.

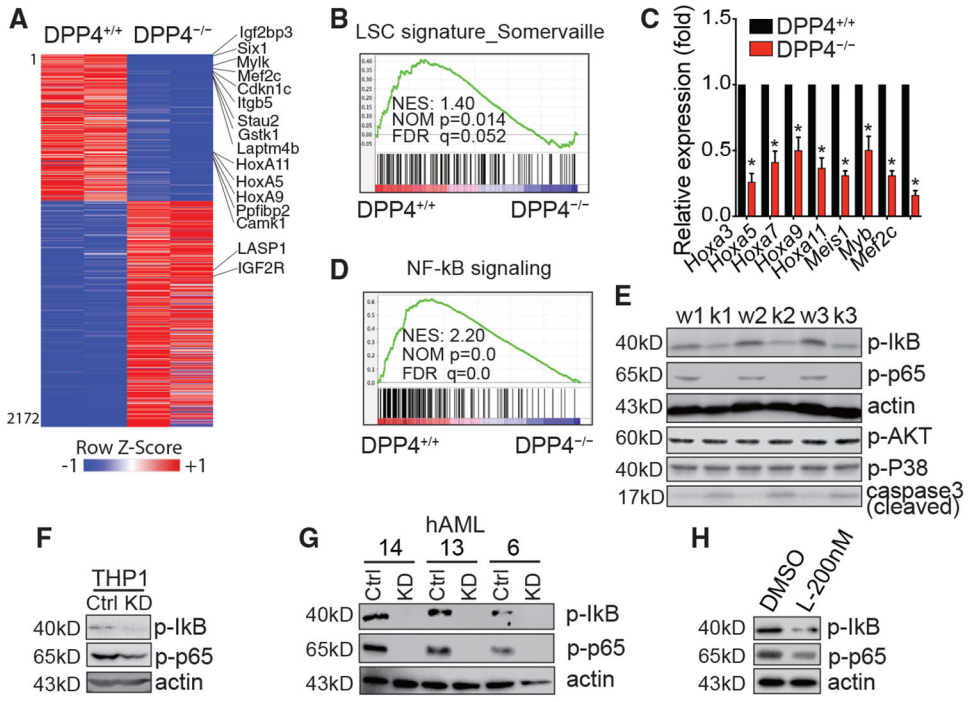

Figure 6. NF-κB activation mediates DPP4-initiated intracellular effects on AML-SCs

(A) Heatmap of 2,172 differentially expressed genes from RNA-seq (n = 2 *DPP4*$^{+/+}$ or *DPP4*$^{-/-}$ BM AML cells, red is higher and blue is lower expression).

(B) Gene set enrichment analysis (GSEA) plot evaluating changes in leukemia initiation/maintenance gene signatures upon DPP4 signaling depletion in *DPP4*$^{+/+}$ and *DPP4*$^{-/-}$ MLL-AF9 AML cells. NES, normalized enrichment score; NOM p, normal p value; FDR q, false discovery rate q value.

(C) Bar graphs compare the change in expression levels of the indicated transcripts in *DPP4*$^{+/+}$ and *DPP4*$^{-/-}$ MLL-AF9 AML cells. All transcripts levels were normalized to levels of *actin* expression (n = 3 wells).

(D) GSEA plot shows that DPP4 deletion negatively coordinates NF-κB signaling in AML cells.

(E) Comparison of p-IκB, p-p65, p-AKT, p-P38, and cleaved caspase3 protein levels in *DPP4*$^{-/-}$ (k, KO) and *DPP4*$^{+/+}$ (w, WT) MLL-AF9^{+} BM cells from each of 3 primary transplanted mice.

(F–H) Immunoblotting of p-IκB and p-p65 in scramble (control [Ctrl])- and DPP4 shRNA (KD)-treated THP1 cells (F) and hAML cells (G, samples #14, #13, and #6) and in DMSO- or Lgp (200 nM)-treated hAML cells (H, sample #14).

Error bars, SEM. *p < 0.05, Data were analyzed using two-tailed Student's t test; when comparing 3 or more groups, one-way or two-way ANOVA was used with Fisher's test for post-hoc analyses.

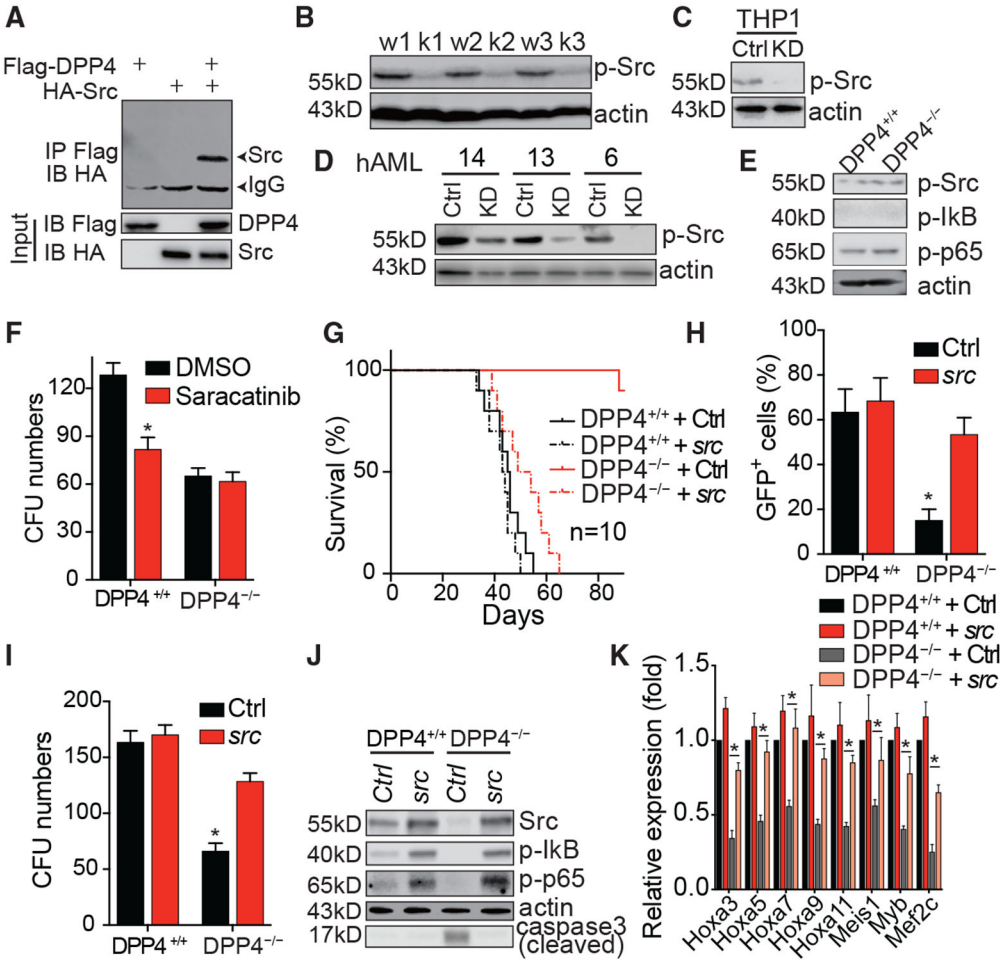

Figure 7. Src is essential to the regulation by DPP4-NF-κB axis of AML development

(A) DPP4 binds to Src in transfected 293T cells. FLAG-tagged DPP4 and/or hemagglutinin (HA)-tagged Src was overexpressed in 293T cells. FLAG antibody was used to precipitate DPP4 protein, and the FLAG or HA antibodies were used in WB.

(B–D) Comparison of p-Src levels in *DPP4*$^{-/-}$ (k) and *DPP4*$^{+/+}$ (w) MLL-AF9^{+} BM cells from each of 3 primary transplanted mice (B) and scramble- (Ctrl) and DPP4 shRNA (KD)-treated THP1 cells (C) or hAML cells (samples #14, #13, and #6) (D) determined by WB.

(E) p-Src, p-IκB, and p-p65 in non-AML *DPP4*$^{+/+}$ and *DPP4*$^{-/-}$ BM cells were determined by WB.

(F) Comparison of colony-forming activity of *DPP4*$^{+/+}$ and *DPP4*$^{-/-}$ MLL-AF9 AML cells upon saracatinib (5 μM) treatment (2,000 cells/well, n = 3 wells).

(G) Retrovirally expressed src reversed the DPP4 knockout phenotype in transplantation assay. MLL-AF9^{+}, *DPP4*$^{+/+}$, or *DPP4*$^{-/-}$ BM cells in primarily transplanted mice were collected at 40 days and were infected with *Src*-encoding or control virus. Survival curves of mice transplanted with 3,000 of these ectopically *src*-expressing or control cells (n = 10 mice; $p < 0.0001$, log rank test).

(H) Proportions of retrovirus infected (GFP^{+}) AML cells in PB of secondary recipient mice after 28 days of transplantation (n = 10 mice).

(I) Retrovirally expressed src increased CFU numbers of *DPP4*$^{-/-}$ AML cells compared with cells that were infected with control virus in colonyforming assays (2,000 cells/well, n = 3 wells).

(J) WB showing the activity of IκB and p65 in *DPP4*$^{+/+}$ and *DPP4*$^{-/-}$ AML cells upon Src overexpression.

(K) Bar graphs compare the change in expression levels of the indicated transcripts in *DPP4*$^{-/-}$ MLL-AF9 AML cells ectopically expressing either control or *src* gene (n = 3 wells).

Error bars, SEM. *p < 0.05. Data were analyzed using two-tailed Student's t test; when comparing 3 or more groups, one-way or two-way ANOVA was used with Fisher's test for post-hoc analyses, except that the p value of (G) was derived from log rank test.

KEY RESOURCES TABLE

REAGENT or RESOURCE	SOURCE	IDENTIFIER
Antibodies		
Anti-mCD3e-PE/Cyanine5	Biolegend	Cat#100310; RRID:AB_312675
Anti-mLy-6G/Ly-6C (Gr-1)-PE/Cyanine5	Biolegend	Cat#108410; RRID:AB_313375
Anti-mCD11b-PE/Cyanine5	Biolegend	Cat#101210; RRID: AB_312793
Anti-mCD45R-PE/Cyanine5	Biolegend	Cat#103210; RRID: AB_312995
Anti-mTer-119-PE/Cyanine5	Biolegend	Cat#116210; RRID: AB_313711
Anti-mCD117 (c-Kit)-APC	Biolegend	Cat#105812; RRID: AB_313221
Anti-mSca-1-PE-cy7	Biolegend	Cat#108114; RRID: AB_493596
Anti-mCD150-PE	Biolegend	Cat#115904; RRID: AB_313683
Anti-mCD48-APC/Cyanine7	Biolegend	Cat#103432; RRID: AB_2561463
Anti-mKi67-FITC	Biolegend	Cat#652410; RRID: AB_2562141
Hoechst34580	BD Pharmingen	Cat#565877; RRID:AB_2869723
Anti-mCD16/32-PE	Biolegend	Cat#101308; RRID: AB_312807
Anti-mCD34-FITC	eBioscience	Cat#11-0341-82; RRID: AB_465021
Anti-mCD127-APC/Cyanine7	Biolegend	Cat#135040; RRID: AB_2566161
Anti-mCD135-Brilliant Violet421	Biolegend	Cat#135314; RRID: AB_2562339
Anti-hCD45-PE	Biolegend	Cat#304039; RRID: AB_2562057
Annexin V	Biolegend	Cat#640941; RRID: AB_2616657
7-AAD	Biolegend	Cat#420404
PI	Biolegend	Cat#421301
Bacterial and virus strains		
pLentiLoxp3.7	Addgene, Watertown MA	# 11795
MSCV-MLL-AF9-IRES- YFP/GFP	Addgene	#71443
Mig-AML1-ETO9a	Addgene	#12433
MSCV-SRC-IRES-GFP		This manuscript
Flag-DPP4		This manuscript
MSCV-IP N-HAonly SRC	Addgene	#35017
Biological samples		
Primary human AML samples	Ellis Fischel Cancer Center, University of Missouri	N/A
Human peripheral blood samples	Ellis Fischel Cancer Center, University of Missouri	N/A
Chemicals, peptides, and recombinant proteins		
5-Fluorouracil	Sigma	F6627
Protease inhibitor cocktail	Roche Diagnostics	
H-Ala-Pro-AFC	Bachem Americas	I-1680.0050BA
Ara-C	Sigma-Aldrich	147-94-4
Linagliptin	MedChemExpress	HY-10284
Vildagliptin	MedChemExpress	HY-14291
EDTA	Sigma-Aldrich	10378-23-1

REAGENT or RESOURCE	SOURCE	IDENTIFIER
4% phosphate-buffered formalin	Sigma-Aldrich	1.00496
Critical commercial assays		
mycoplasma contamination kit	R&D Systems	CUL001B
Foxp3/Transcription factor staining set	eBioscience	00-5523-00
miRNeasy Mini Kit	QIAGEN	217084
Qubit HS RNA assay kit	Invitrogen	Q32852
Qubit HS dsDNA assay kit	Invitrogen	Q32851
One Step RT-PCR kit	QIAGEN	210212
Shandon™ Rapid-Chrome H & E Frozen Section Staining Kit	Thermo Scientific	Epredia™ 9990001
Deposited data		
RNA-seq datasets	This study	“SRA database: SRP323430”
Experimental models: Cell lines		
THP-1	ATCC	TIB-202
MV4-11	ATCC	CRL-9591
K562	ATCC	CCL-243
697	DSMZ	ACC 42
Kasumi2	DSMZ	ACC 526
Sup15B	ATCC	CRL-1929
KOPN8	DSMZ	ACC 552
RCH-ACV	DSMZ	ACC 548
REH	ATCC	CRL-8286
MHH-Call-2	DSMZ	ACC 341
NALM-6	ATCC	CRL-3273
MOLM	DSMZ	ACC 554
MM6	DSMZ	ACC 124
Kasumi1	ATCC	CRL-2724
U937	ATCC	CRL-1593.2
Experimental models: Organisms/strains		
C57 BL/6	Charles River	N/A
CD45.2	Charles River	N/A
CD45.1	Charles River	N/A
C57Bl/6NTac-DPP4tm1a Wtsi/Ics	European Mouse Mutant Cell Repository	N/A
129S4/Bl6-Gt(ROSA)26Sortm2 (FLP*)Sor/J	Jackson	JAX: 012930
Vav-iCre	Jackson	JAX: 018968
Oligonucleotides		
Mouse primers for qPCR, see Method details	Sigma	N/A
Human primers for qPCR, see Method details	Sigma	N/A
Software and algorithms		
GraphPad Prism version 7.0	GraphPad software	
Flowjo v10	BD	https://www.flowjo.com/solutions/flowjo

REAGENT or RESOURCE	SOURCE	IDENTIFIER
Quant StudioTM Real-Time PCR software v1.3	Applied Biosystems	https://www.thermofisher.com/de/de/home/global/forms/life-science/quantstudio-6-7-flex-software.html
edgeR		http://software.broadinstitute.org/gsea/index.jsp
hierarchical clustering		https://software.broadinstitute.org/morpheus
GSEA version 2.2.0	Mootha et al., 2003[55]	